

LOW BACK BIOMECHANICAL ANALYSIS OF ISOMERIC PUSHING AND PULLING TASKS

PATRICK LEE

Thesis presented to

The faculty of the Virginia Polytechnic Institute and State University

in partial fulfillment of the requirements for the degree of

Master of Science

in

Mechanical Engineering

Kevin P. Granata, Ph.D., Chair

Michael Madigan, Ph.D.

Stefan Duma, Ph.D.

January 3, 2005

Blacksburg, Virginia

Keywords: Low-Back, Co-contraction, Push, Stiffness, Spine, Stability

LOW BACK BIOMECHANICAL ANALYSIS OF ISOMERIC PUSHING AND PULLING TASKS

Patrick Lee

(ABSTRACT)

Few studies have investigated the neuromuscular recruitment and stabilizing control of the spine during pushing and pulling exertions. Past theoretical investigation suggest that co-contraction of the of the paraspinal muscles is necessary to stabilize the spine during pushing exertions. We hypothesized greater levels of co-contraction during pushing exertions. Co-contraction of trunk musculature was quantified during isometric pushing and pulling tasks. The mean value of co-contraction during pushing was two-fold greater ($p < 0.01$) than during extension.

Co-contraction has been shown to increase the stiffness of the ankle but this effect has not been demonstrated in the trunk. Trunk stiffness was measured as a function of co-activation during extension exertions. Results demonstrate trunk stiffness was significantly ($p < 0.01$) greater with co-activation.

Trunk stiffness was calculated during isometric pushing and pulling exertions. We hypothesized trunk stiffness would be greater during pushing tasks due to increased levels of co-contraction to maintain stability of the spine. Results demonstrate trunk stiffness was significantly ($p < 0.05$) greater during pushing compared to pulling exertions.

Results suggest that trunk isometric pushing tasks require more co-contraction than pulling tasks enable to maintain spinal stability. Greater levels of co-contraction

during pushing exertions caused trunk stiffness to be greater during pushing compared to pulling tasks. Results may indicate greater risk of spinal instability from motor control error during pushing tasks than pulling exertions. Future studies need to consider co-contraction and neuromuscular control of spinal stability when evaluating the biomechanical risks of pushing and pulling tasks.

ACKNOWLEDGEMENTS

The research described here was made possible through contributions from lab mates, family members, and friends.

Students of the Musculoskeletal Biomechanics Lab

Special thanks goes to Ellen Rogers and Greg Slota for their help with data collections. Shawn Russell for his knowledge of lab equipment, specifically the servomotor. Kevin Moorhouse for his model development.

Dr. Granata

For his excellent guidance as my advisor and for giving me a chance to be successful. He was influential in making me a more capable engineer.

Dr. Madigan

For being a friend and a co-worker.

My family

My family has provided support for me through this process and throughout my whole life. Thanks to my parents for stressing the importance of education. Also special thanks to my sister Jeanine, my brother Michael, and my sister in-law Kim for their support.

Ellen

For helping me more than you can ever imagine

TABLE OF CONTENTS

ABSTRACT	ii
ACKNOWLEDGEMENTS	iv
TABLE OF CONTENTS	v
LIST OF FIGURES	vii
LIST OF TABLES	ix
 CHAPTER 1 – INTRODUCTION	 1
Hypotheses	3
Specific Aims	3
 CHAPTER 2 – BACKGROUND	 4
2.1 Electromyography	4
2.1.1 EMG Basics	4
2.1.2 EMG Processing	4
2.1.3 EMG Placement	6
2.1.4 Antagonistic Co-contraction and Co-activation	6
2.2 Quantitative Assessment of Co-Contraction	7
2.2.1 Biomechanical Modeling	7
2.2.2 EMG-Assisted Determination of Muscle Force	9
2.2.3 Co-Contraction Analysis	10
2.3 System Identification	12
2.3.1 System Identification for Estimation of Joint Stiffness	12
2.3.2 Linear Time-Invariant Systems	12
2.3.3 Convolution	14
2.3.4 Correlation Function Analysis	14
2.3.5 Parameterization of Nonparametric Models	18
2.4 References	21
 CHAPTER 3 - CO-CONTRACTION RECRUITMENT AND SPINAL LOAD DURING ISOMETRIC TRUNK FLEXION	 25
3.1 Introduction	28
3.2 Methods	31
3.3 Results	35
3.4 Discussion	37
3.5 Acknowledgement	42

3.6 Appendix	43
3.7 References	47
3.8 Figures and Tables	51
CHAPTER 4 – ACTIVE TRUNK STIFFNESS INCREASES WITH CO-CONTRACTION	56
4.1 Introduction	58
4.2 Methods	59
4.3 Results	63
4.4 Discussion	65
4.5 Acknowledgement	68
4.6 References	69
4.7 Figures and Tables	72
CHAPTER 5 - ACTIVE TRUNK STIFFNESS DURING VOLUNTARY ISOMETRIC FLEXION AND EXTENSION EXERTIONS	77
5.1 Introduction	79
5.2 Methods	81
5.3 Results	85
5.4 Discussion	87
5.5 Conclusions	90
5.6 Acknowledgement	91
5.7 References	91
5.8 Figures	94
CONCLUSIONS	99
APPENDICES	101
A. IRB Approval Form	101
B. Consent Form	102
C. Data Collection Sheets	104
VITA	106

LIST OF FIGURES

CHAPTER 2

- Figure 2.1. Typical raw EMG activity of muscle during periods of muscle activation and periods of rest recorded by a surface electrode 5
- Figure 2.2. Schematic representation of the EMG placement of the four major trunk muscle groups 6
- Figure 2.3. The triceps promote elbow extension although co-contraction of the biceps will be apparent despite the fact that it inhibits elbow extension 7
- Figure 2.4. Single degree of freedom pendulum 12
- Figure 2.5. Typical IRF relating trunk displacement to the applied trunk force and the superimposed second order fit 19

CHAPTER 3

- Figure 3.1. Experimental setup 52
- Figure 3.2. Schematic representation of trunk musculature used to quantify trunk co-contraction during trunk flexion and extension 53
- Figure 3.3. Co-contraction levels were significantly greater during flexion exertions ($p < 0.01$) 54

CHAPTER 4

- Figure 4.1. Experimental setup 73
- Figure 4.2. IRFs relating trunk displacement to the applied trunk force during maximal and minimal co-activation and the superimposed second-order least-mean-squares fit 74

- Figure 4.3. Comparison of EMG activity with co-activation 75

CHAPTER 5

- Figure 5.1. Experimental setup 95
- Figure 5.2. Typical IRF relating trunk displacement to the applied trunk force 96

Figure 5.3. Normalized EMG activity was greater in three of the four bilateral muscle groups during flexion than during extension exertions 97

Figure 5.4. Trunk stiffness was significantly greater during flexion exertions than during extension exertions 98

LIST OF TABLES

CHAPTER 3

Table 3.1. Model predicted spinal compression (N) from total muscle forces, task muscle forces, and co-contraction during all three load levels	55
---	----

CHAPTER 4

Table 4.1. Trunk stiffness during active voluntary exertions	76
--	----

CHAPTER 1 - INTRODUCTION

Low-back disorders (LBDs) are the most prevalent source of musculoskeletal disability and one of the most significant musculoskeletal problems in the United States. LBDs are the leading cause of lost work days and the most costly occupational safety and health problem facing industry. Epidemiologic studies have identified manual material handling (MMH) tasks with high risk of occupational-related LBDs¹⁹. Push-pull exertions now account for nearly half of MMH² as industry is rapidly changing from lifting tasks to pushing and pulling tasks. Research has identified pushing and pulling as a major LBD risk factor, accounting for 20% of injury claims^{9;14}. Trunk biomechanics represents a significant predictor of occupational LBD risk¹⁹ but little is known regarding biomechanical risks of industrial pushing and pulling tasks. Clearly, there is a significant need to quantify the biomechanical demands placed on the body during pushing and pulling tasks to control the prevalence of occupational LBD.

The primary muscle groups recruited for generation of a trunk flexion exertion during a pushing task are the recti abdomini (RA) and the external obliques (EO). However, it may be necessary to also recruit the lumbar paraspinal (LP) muscles during pushing exertions to guard against global and local instability of the spine⁴ despite the fact that they provide no mechanical potential for the generation of a flexion moment. Conversely, recruitment of the LPs are required to generate trunk extension during a pull or lift task thereby contributing stability to the spine. During a pull or lift task spinal stability may be augmented with low levels of antagonistic co-contraction⁴. Choi⁶ found higher co-contraction in the muscles surrounding the cervical spine during neck flexion then extension using an EMG-assisted optimization procedure. However, we are aware

of no studies to empirically quantify-lumbar co-contraction during push/pull tasks. Increased levels of co-contraction are known to increase the stiffness around a joint ¹³. If flexion exertions are associated with greater co-contraction than extension exertions then one should expect greater trunk stiffness during flexion exertions. However, past investigations have found no difference in trunk stiffness between flexion and extension exertions ^{8;24}.

There are three goals of this study. First, empirically quantify and compare co-contraction during trunk flexion exertions versus trunk extension exertions. Second, document that trunk stiffness increases with co-contraction in the torso musculature. Third, empirically measure and compare trunk stiffness during trunk flexion exertions versus trunk extension exertions. This thesis will present each goal (chapter) in a separate formatted manuscript and submitted for publication in peer-reviewed biomechanical journals.

HYPOTHESES

1. Co-contraction of trunk muscles will be greater during flexion extensions then during extension exertions (Chapter 3).
2. Co-contraction of the trunk musculature contributes to increased trunk stiffness (Chapter 4).
3. Trunk stiffness will be greater during flexion then extension exertions (Chapter 5).

SPECIFIC AIMS

1. a) Measure trunk muscle activation (EMG) during trunk flexion and extension exertions.
b) Implement a computational model to quantify torso muscle co-contraction from measured EMG data.
c) Compare torso muscle co-contraction during flexion exertions versus co-contraction during trunk extension exertions.
2. Quantify the influence of co-contraction on trunk stiffness during voluntary isometric extension exertions.
3. Measure and compare trunk stiffness during flexion and extension exertions computationally.

CHAPTER 2 - BACKGROUND

2.1 Electromyography

2.1.1 EMG Basics

When a muscle is stimulated by a nerve, neurotransmitters such as acetylcholine induce Ca^{2+} release from sarcoplasmic reticulum that surround each muscle fiber. This triggers an opening of the voltage dependent Na^{+} and K^{+} channels, creating a depolarization front called an action potential, which travels through the length of the muscle fiber. An action potential can be characterized as a biphasic, and sometimes triphasic, waveform similar to a nerve. As the waveform travels the length of the muscle fiber, the change in electric potential in or around the surrounding muscle due to depolarization of the cell membrane can be measured using differential electrodes parallel to the length of the fiber. This is commonly referred to as electromyography (EMG). Single muscle fiber activity can be recorded by means of intra-muscular electrodes. Non-invasive surface electrodes can be used to record composite activity from muscle fiber groups in the vicinity of the electrode to represent whole muscle recruitment. In this study, overall recruitment patterns of muscle groups are more of interest than the activity of a single fiber. Therefore surface EMG is used to record the summation of action potentials of a muscle group underlying the skin where the electrodes are placed. Proper processing of the raw EMG along with successful placement of EMG is necessary for appropriate interpretation of myoelectric activity.

2.1.2 EMG Processing

The goal of EMG measurement is to achieve insight into muscle recruitment patterns. Therefore the EMG signal must be appropriately conditioned and processed to represent muscle

activation. Raw surface EMG recorded during periods of muscle activation appears to be chaotic in character with varying amplitude (Figure 2.1) even though it truly is the superposition of action potentials from multiple muscle fibers within a muscle group. The first step in processing raw EMG is to amplify and band-pass filter the differential signal between 20 and 500 Hz by the EMG hardware. This is to eliminate low frequency motion artifacts and to remove high frequency noise above 500Hz. To prevent aliasing when the signal is acquired it is necessary to record the data at collection frequencies greater than 1000 Hz. The signal is full-wave rectified to translate the raw EMG into a single polarity. Using software the signal is low-pass filtered and smoothed, at or below 30 Hz. The Butterworth filter also serves the purpose of replicating the second order response of the muscle to the impulses provided the action potentials²³. Collected and processed EMG are normalized to a maximum voluntary contraction (MVC) of each muscle to compare myoelectric activity of different muscles and individuals.

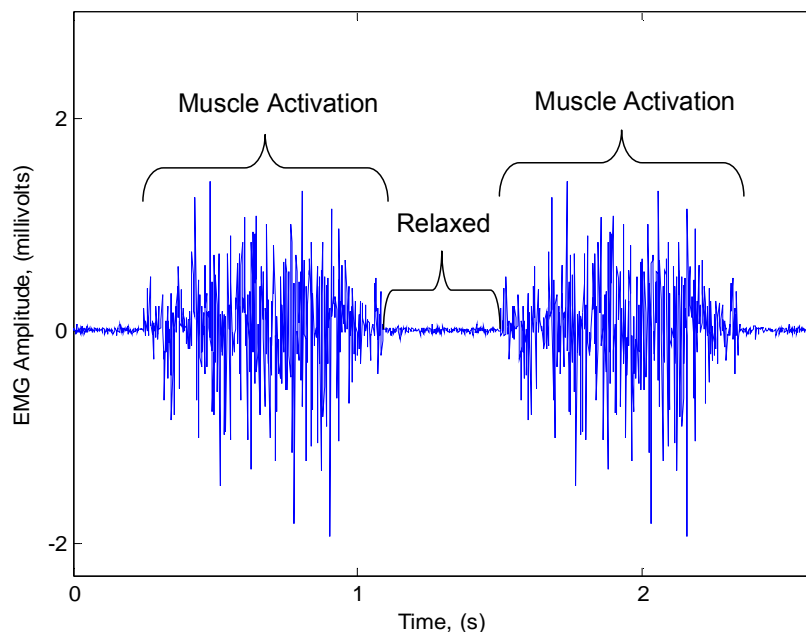


Figure 2.1. Typical raw EMG activity of muscle during periods of muscle activation and periods of rest, recorded by a surface EMG electrode.

2.1.3 EMG Placement

In research interested in muscle activity of a body segment, EMG are commonly collected from all of the major muscle groups within the segment. For research of the lumbar torso measured trunk muscles typically reported in the literature¹² include the left and right recti abdomini (RA), lumbar paraspinal (LP), internal oblique (IO), and external oblique (EO). These four muscle groups constitute the four major muscle groups of the lower back. Electrodes for the RA are placed 3 cm lateral and 2 cm superior to the umbilicus; LP 4 cm lateral to the L3 spinous process; posterior IO 8 cm lateral to the midline within the lumbar triangle at a 45°; and EO 10 cm lateral to the umbilicus with an orientation of 45° to vertical²¹ (Figure 2.2).

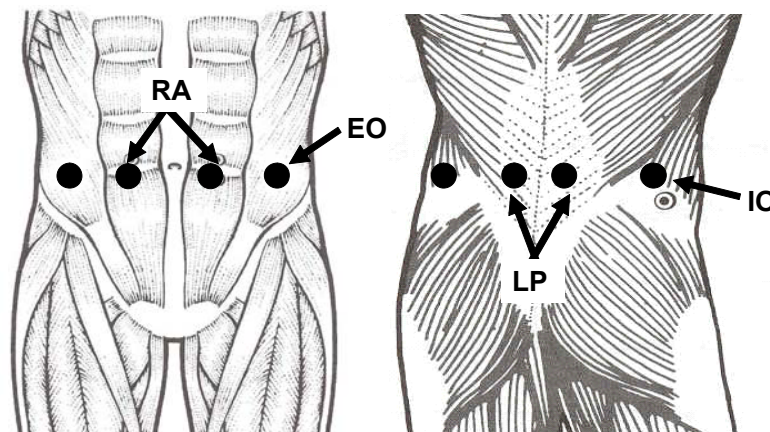
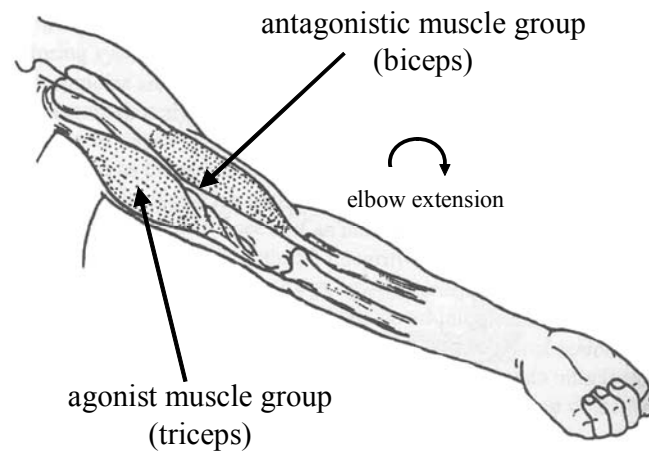


Figure 2.2. Schematic representation of the EMG placement of the four major trunk muscle groups (left and right rectus abdominus, external obliques, lumbar paraspinals, and internal obliques).

2.1.4 Antagonistic Co-activation and Co-contraction

Muscles work in agonist and antagonist pairs in the musculoskeletal system. Agonist muscles are arranged in groups around joints so that their contraction is responsible for promoting movement of a body segment. Antagonist activity tends to oppose the movement and provide no mechanical potential to contribute to the displacement output. For example, during elbow rotation from a flexed to an extended position the triceps promote movement of the elbow

towards full extension while the biceps oppose this action (Figure 2.3). Activity of the antagonistic muscle is a common occurrence in human body movement about a joint, this phenomena is known as antagonistic co-activation⁵. Recognizing that muscle force increases with activation¹⁶, antagonistic muscle force is higher during co-activation. This is commonly referred to antagonistic co-contraction.



From Chaffin, DB et al (1999) *Occupational Biomechanics*, Fig 2.26

Figure 2.3. The triceps promote elbow extension although co-contraction of the biceps will be apparent despite the fact that it inhibits elbow extension.

2.2 Quantitative Assessment of Co-contraction

2.2.1 Biomechanical Modeling

Estimation of muscle forces from a biomechanical model with some level of anatomic accuracy cannot be uniquely solved using traditional mechanics because of the indeterminacy problem. There are many more muscles than degrees of freedom for any anatomical joint since muscle forces are commonly unknown in biomechanical problems. Therefore, there is no unique determinate solution of muscle forces. One method for resolving this issue is to reduce the

number of unknowns, i.e. by using muscle equivalents. However this limits biofidelity. Lee et al²⁰ computed spinal compression from a biomechanical model of the trunk incorporating only one trunk muscle. This model did not consider co-contraction. Lee acknowledges that “assuming that only one muscle is active at one time to stabilize the torso may not be appropriate for the estimation of muscle forces in the lower back”. Another approach is to collect EMG and estimate muscle force using a well documented EMG-force relationship¹¹. Briefly, EMG is normalized to the highest amplitude during maximum voluntary contractions. Further conversion of muscle activity to force requires an incorporation of muscle cross sectional area, muscle length, and shortening/lengthening velocity.

Optimization is another known method to overcome indeterminacy. Optimization finds the minimum of an objective function subject to one or more constraints. For example, the force of the biceps brachii (F_1) and brachialis (F_2) muscle can be found using optimization given the moment about the elbow (M_E) caused by these two muscles and their respective moment arms (r_1, r_2).

$$M_E = r_1 F_1 + r_2 F_2 \quad (2.1)$$

A common objective function is to minimize the sum of the two forces (equation 2.2) subject to the constraint that summation of the moment due to each muscle force are equal to the total moment about the elbow (equation 2.3). A boundary constraint may be that each muscle must be greater than zero because muscles only work tension (equation 2.4).

$$\min \sum F_i \quad (2.2)$$

$$\sum r_i F_i = M_E \quad (2.3)$$

$$F_i \geq 0 \quad (2.4)$$

Predicted muscle force is dependent on the objective function. Optimization generally doesn't account for antagonistic co-contraction. Another limitation of optimization is that it fails to fully represent inter-subject variability. However, a hybrid approach of EMG and an optimization model can be used to quantify co-contraction and account for inter-subject variability.

2.2.2 EMG-Assisted Determination of Muscle Force

Quantification of co-contraction in cervical musculature has been successfully achieved through the use of an EMG-assisted optimization model⁶. Muscle forces were decomposed into a task subset and a co-contraction subset of forces. The task subset represented the minimal muscle force needed to maintain equilibrium during the exertion, while the co-contraction subset represented the muscle forces due to antagonistic co-contraction. The summation of the task and co-contraction subsets equals the total muscle forces calculated from the EMG-force relationship.

Inputs to the model were EMG data and measured external loads. EMG were collected, processed, and normalized to a maximum voluntary contraction (MVC) for the major cervical musculature. MVC were taken as the largest amplitude of EMG data from steady-state three second maximum isometric flexion, extension, and left and right-lateral cervical twisting exertions. External loads were calculated about the C5/C4 joint using inverse dynamics from recorded reaction forces. Estimated weights of the head were established from published anthropometric data.

To construct the model muscle origins, insertions, and cross sectional areas of the cervical muscles were established from published anatomy. The moment generating capacity of

each muscle was determined from the vector product between the unit vector direction of muscle force, \hat{F}_i , and the muscle origin, r_i , for each muscle $i = 1..12$. This was scaled by the muscle force magnitude, F_i , to determine muscle moment. The sum of muscle moments must achieve equilibrium with respect to the measured external moments (equation 2.5).

$$M_{ext} = \sum_{i=1}^n F_i \{r_i \times \hat{F}_i\} \quad n = 12 \quad (2.5)$$

Muscle force (equation 2.6) was assumed to have a power relationship with normalized EMG ^{7,25}.

$$F_i = \left(\frac{EMG}{EMG_{max}} \right)^{1/1.3} a_i G_i \quad (2.6)$$

where F_i is the i^{th} muscle force (N), a_i is the i^{th} muscle cross-sectional area (m^2), EMG/EMG_{max} is the normalized muscle activity, and G_i is muscle Gain. Gain represents the muscle force capacity per unit cross-sectional area and were required to be calibrated for each subject. Each subject had the same value of gain for each muscle.

This procedure allowed for a set of muscle forces to be estimated from measured EMG and kinetic loads. Decomposition of this set of muscle forces into a task subset and co-contraction subset is discussed next.

2.2.3 Co-contraction Analysis

Note that muscle forces determined from the EMG-assisted approach include components necessary to achieve equilibrium plus the effects of co-contraction, F_{i_Total} . Co-contraction was determined by comparing F_{i_Total} with values necessary for equilibrium. The set of muscle activations and associated forces (equation 2.6) necessary to achieve equilibrium without co-

contraction, F_{i_Equil} , were estimated by means of linear programming. Specifically, the set of muscle activations were determined to minimize the sum of squared muscle force with equilibrium equality constraint (equation 2.5). Note that the objective function results in muscle forces sufficient for equilibrium but with no co-contraction. The Gain contributes to the force magnitude during this process and was therefore calibrated prior to estimation of muscle activation by setting it equal to the Gain value computed from the EMG-assisted model described above. The components of muscle force attributed to co-contraction were determined by comparing the two sets of muscle forces,

$$F_{i_Co-Contr} = F_{i_Total} - F_{i_Equil} \quad (2.7)$$

Co-contraction was expressed as the percentage total muscle force, i.e. the ratio of the sum of $F_{i_Co-Contr}$ versus the sum of F_{i_Total} .

$$Co-contraction = 100 \left\{ \frac{\sum_{i=1}^n F_{i_Co-Contr}}{\sum_{i=1}^n F_{i_Total}} \right\} \quad (2.8)$$

Spinal load was computed as the vector sum of muscle forces and included components of spinal load attributed to co-contraction and spinal load attributed to equilibrium muscle forces.

Using this methodology the contribution of muscle co-contraction can be quantified along with co-contraction's contribution on spinal load. Choi⁶ observed a three-fold increase in co-contraction from neck extension (8-16%) to flexion (30-41%) in cervical musculature. The amount of spinal compression due to co-contraction during neck flexion exertions was an average of 38.9%. It is believed this procedure can be used to quantify co-contraction in lumbar musculature during trunk movement about the L5/S1 joint to provide insight into antagonistic co-contraction's influence on spinal load in the lumbar back.

2.3 System Identification

2.3.1 System Identification for Estimation of Joint Stiffness

Dynamics deals with the relation between forces acting on a body and the resulting movement. Musculoskeletal joint dynamics are generally non-linear. However, for small displacements about a prescribed operating point, the dynamic behavior is adequately represented by a linear second-order model¹⁸. In other words, for small force or angular perturbations about an approximately constant trunk moment and posture the system dynamics can be represented as a linear second-order system. In this study, trunk stiffness was calculated using this methodology and is described in detail in the rest of the section.

2.3.2 Linear Time-Invariant Systems

To understand physical dynamics, a mathematical model is created. Such models can be called a system, a process that will behave a certain way given an input and an initial state. Some systems are highly complex, such as the weather, where the sunlight and ocean currents can be seen as inputs and snowfall can be seen as an output. Other systems are simpler such as a one segment pendulum (Figure 2.4).

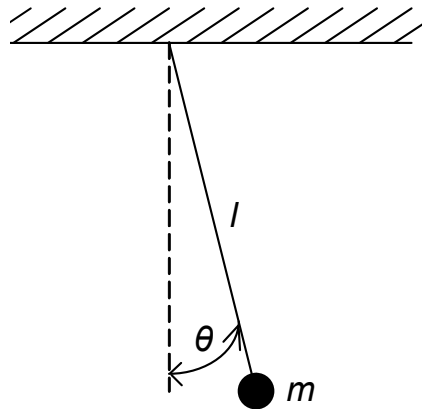


Figure 2.4. Single degree of freedom pendulum.

The output of this system, i.e. angular displacement of a pendulum from a resting position given a unit impulse, is known as the impulse response function (IRF).

The IRF for this system can simply be written as

$$\theta(t) = \sin\left(\sqrt{\frac{g}{l}}t\right) \quad 2.9$$

where g is the acceleration due to gravity, $\theta(t)$ is angular displacement of the pendulum measured from vertical as a function of time, and l is the length of the cord with an attached mass, m .

System identification techniques have been developed to understand system dynamics. These techniques are especially useful for linear time-invariant (LTI) systems. A linear time-invariant (LTI) system is defined as a system that has the properties of scalability, additivity, and time-invariance. In the case of a system with input $x(t)$ and output $y(t)$, the output can be written as an operator function of the input, or $f(x(t)) = y(t)$. A system is said to be scalable or linear if a multiplying a factor to the input results in output that is multiplied by the same amount.

$$f(ax(t)) = ay(t) \quad 2.10$$

A system is said to be additive (or superimposable) if input $x_1(t)$ results in output $y_1(t)$, and input $x_2(t)$ results in output $y_2(t)$, then given input of the sum of $x_1(t)$ and $x_2(t)$, the system output will be the sum of $y_1(t)$ and $y_2(t)$.

$$f(x_1(t) + x_2(t)) = y_1(t) + y_2(t) \quad 2.11$$

A system is said to be time-invariant if the time shift of input results in identical time shift of the output.

$$f(x(t-s)) = y(t-s) \quad 2.12$$

Few systems are truly linear and time-invariant, but approximating such systems is reasonable and has been used to describe trunk stiffness²² and stretch reflex dynamics¹⁷.

2.3.3 Convolution

The input $x(t)$ signal of a system can be interpreted as a string of very short pulses as shown in equation 2.13 , where δ is the pulse height, $\delta=1/\Delta$, and Δ is the pulse width.

$$x(t) = \sum_{k=-\infty}^{\infty} x(k\Delta) \delta_{\Delta}(t-k\Delta) \Delta \quad 2.13$$

As $\lim \Delta \rightarrow 0$, the above sum can be written as an integral of the signal value multiplied by a delta function, an infinitely high and short pulse with area of unity (equation 2.14).

$$x(t) = \int_{t=-\infty}^{\infty} x(\tau) \delta(t-\tau) d\tau . \quad 2.14$$

A linear time-invariant system can be described using its response to a delta function, known as the impulse response. For each instant in time the signal at that point can be considered as a delta function, and it will result in an impulse response. Next moment in time the signal will result in another impulse. Since the system is additive, the impulse responses can be added up over the time from the initial to final limit. Then the output of the system will be the sum of all impulse responses. This mathematical process is called convolution (equation 2.20), where output $y(t)$ can be described by the IRF, $h(t)$ convolved (notated with $*$) with input $x(t)$.

$$y(t) = \int_{-\infty}^{\infty} x(\tau) h(t-\tau) d\tau = x(t) * h(t) \quad 2.15$$

2.3.4 Correlation Function Analysis

A linear system can be represented as either a parametric or nonparametric filter. A nonparametric form can be represented by a curve and a parametric form can be represented by an equation. Nonparametric models use descriptions such as an IRF or a frequency response function that make no assumptions about systems structure or order. They are well adapted to

the study of unknown systems. Parametric models describe system behavior in terms of an analytic expression¹⁸. Parametric modeling is only successful if the analytical expression or model structure is selected appropriately to represent the nonparametric system behavior. This may be done using a priori knowledge about the dynamics of the components of the systems. In this study, a nonparametric filter is used to determine the IRF of output trunk movement at the T10 level $y(t)$ of the trunk given an input force $x(t)$. Trunk stiffness is then determined by parameterizing the IRF as a second-order system.

Linear nonparametric models have been used to describe joint dynamics^{1;15;22}. For a time-invariant system a nonparametric filter can be represented by a single real vector in the time domain or by a single vector in the frequency domain (transfer function). One time domain approach involves the use of an iterative minimization procedure in which $h(t)$ is repeatedly convolved with the input as in equation 2.19¹⁵. After each convolution $h(t)$ is modified to reduce the sum of squared errors between actual and predicted outputs until the sum of squares can no longer be reduced. This procedure is very slow. The time domain approach used in this study is called correlation function analysis which involves solving a matrix equation in which the input/output (force/angle) cross-correlation function is expressed as a function of the input (force) autocorrelation function and the filter.

The first step for using the correlation function was to express $y(t)$ as a convolution integral of the $x(t)$ and IRF $h(t)$ (equation 2.16). Using the time-invariance property, the input and the output are shifted by r .

$$y(t+r) = \int_{-\infty}^{\infty} x(\tau+r)h(t-\tau)d\tau \quad 2.16$$

Next, both sides are multiplied by $x(r)$ and integrated over r .

$$x(r)y(t+r) = x(r) \int_{-\infty}^{\infty} x(\tau+r)h(t-\tau)d\tau \quad 2.17$$

$$\int_{-\infty}^{\infty} x(r)y(t+r)dr = \int_{-\infty}^{\infty} x(r) \int_{-\infty}^{\infty} h(t-\tau)x(\tau+r)d\tau dr = \int_{-\infty}^{\infty} \int_{-\infty}^{\infty} h(t-\tau)x(r)x(\tau+r)d\tau dr \quad 2.18$$

With manipulation, the integrals on the right hand side can be written as a convolution of IRF and another integral.

$$\begin{aligned} \int_{-\infty}^{\infty} x(r)y(t+r)dr &= \int_{-\infty}^{\infty} \int_{-\infty}^{\infty} h(t-\tau)x(r)x(\tau+r)d\tau dr \\ &= \int_{-\infty}^{\infty} h(t-\tau) \left(\int_{-\infty}^{\infty} x(r)x(\tau+r)dr \right) d\tau \end{aligned} \quad 2.19$$

Using the definition of the correlation function (equation 2.20a,b), equation 2.19 can be written as equation 2.21, where the cross-correlation function between $x(t)$, and $y(t)$, $C_{xy}(t)$, is the convolution of the IRF and the autocorrelation of $x(t)$, $C_{xx}(t)$.

$$C_{xy}(t) = \int_{-\infty}^{\infty} x(\tau)y(t+\tau)d\tau \quad 2.20a$$

$$C_{xx}(t) = \int_{-\infty}^{\infty} x(\tau)x(t+\tau)d\tau \quad 2.20b$$

$$C_{xy}(t) = \int_{-\infty}^{\infty} h(t-\tau)C_{xx}(\tau)d\tau \quad 2.21$$

Equation 2.21 can also be written in discrete time as equation 2.22.

$$C_{xy}(k) = \sum_{i=-\infty}^{\infty} C_{xx}(i)h(k-i) \quad 2.22$$

Equation 2.22 can be then be written in matrix form and solved for H to obtain:

$$H = \frac{1}{\Delta t} C_{xx}^{-1} C_{xy} \quad 2.23$$

where C_{xy} is an $M_2 - M_1 + 1$ length vector whose i^{th} element is $C_{xy}(M_1 + i - 1)$, C_{xx} is an $M_2 - M_1 + 1$ square matrix whose i, j^{th} element is $c_{xx}(i - j)$, and H is an $M_2 - M_1 + 1$ length vector whose i^{th} element is $h(M_1 + i - 1)$. H will be a vector representing the IRF, i.e. trunk displacement which would occur given a single force impulse.

In physical systems it is often unrealistic to ignore process noise, $n(t)$ in the output signal, $y(t)$. The observed signal $z(t)$ becomes $z(t) = y(t) + n(t)$, or

$$z(t) = \int h(\tau)x(t - \tau)d\tau + n(t). \quad 2.24$$

Using correlation functions, this can be written as

$$C_{xz}(t) = \int h(\tau)C_{xx}(t - \tau)d\tau + C_{xn} \quad 2.25$$

where C_{xn} is the cross-correlation function of $x(t)$ and $n(t)$, as defined in equation 2.20a. As long as $x(t)$ and $n(t)$ are not correlated, i.e. noise is not correlated with input, C_{xn} approaches zero, and thus effects of process noise can be reduced. Published techniques illustrate that adding white noise to the input signal will reduce the effect of sample period by decorrelating the noise from the input signal. The magnitude of white noise added is 30% of one standard deviation of the input trunk force. A lower magnitude of white noise was found to be insufficient to reduce the effect of ample size effects while a higher magnitude was found to drown out the input signal.

Several steps are performed to ensure an accurate IRF c. Since the applied trunk force data would need to be sub-sampled from 1000 Hz to 200 Hz to match the trunk displacement data, both signals are filtered using a 75 Hz, low-pass, seventh-order Butterworth filter in software (Matlab, Natick, MA) to avoid aliasing. The two signals are filtered with the same filter to insure no phase shift (time delay) discrepancy between the signals caused by the

filtering. Both applied trunk force and trunk displacement were subtracted from their mean values prior to analysis in order to properly estimate the correlation functions³.

To measure the quality of the IRF estimate, H_{Est} , of the trunk displacement response, the computed IRF was convolved with the measured pseudorandom force sequence to produce an estimate of the trunk displacement, y_{Est} .

$$y_{Est}(t) = \int x(\tau)H_{Est}(t - \tau)d\tau \quad 2.26$$

The equivalence between the predicted and observed displacements was measured in terms of the percentage of displacement variance accounted for (VAF), defined as

$$VAF = 100 \left(1 - \frac{\sum (y(t)_{Meas} - y(t)_{Est})^2}{\sum (y(t)_{Est})^2} \right) \quad 2.27$$

VAF equal to 100% indicates the IRF exactly predicts the measured trunk displacement signal from the input force perturbations.

2.3.5 Parameterization of Nonparametric Models

Previous studies have estimated trunk stiffness by parameterizing the dynamics of the trunk as a second order linear system^{8;10}. Inspection of the IRF shapes from the experiment reveal that the system appears to be very similar to a second-order, underdamped system exhibiting one oscillation (Figure 2.5).

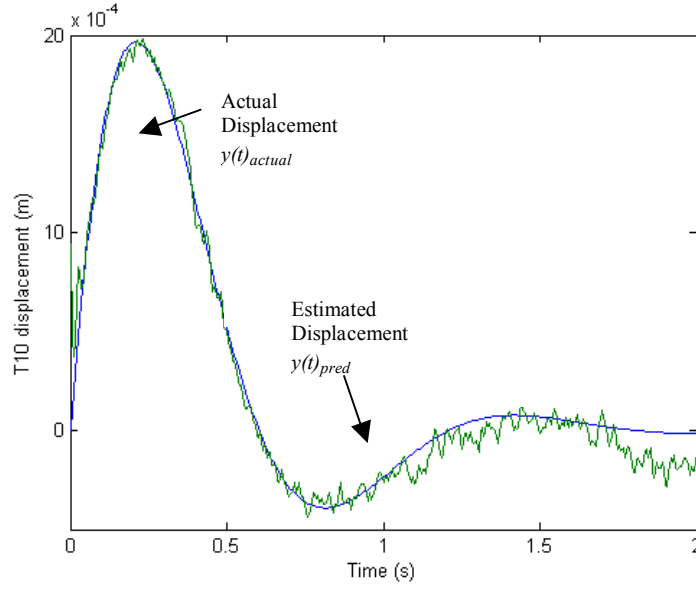


Figure 2.5. Typical IRF relating trunk displacement to the applied trunk force and the superimposed second order fit. This clearly illustrates that a linear second order system can accurately describe trunk dynamics.

The nonparametric IRFs were subsequently parameterized using a second-order system in the time domain of the form:

$$\hat{H}(t) = Ae^{-Bt} \sin(\omega_d t) \quad 2.28$$

where A is the underdamped amplitude, B is the damping coefficient, and ω_d is the damped natural frequency. The values of A, B and ω_d that best approximate the system dynamics can be selected by minimizing the least square error (LSE) between estimated displacement, $y_{pred}(t)$, and calculated nonparametric displacement, $y_{actual}(t)$, (Figure 2.5).

$$LSE = \frac{\sum_t (y_{pred}(t) - y_{actual}(t))^2}{\sum_t (y_{actual}(t))^2} \quad 2.29$$

To calculate the system stiffness it is first necessary to look at the typical Laplace representation of a second order system:

$$\hat{H}(s) = \frac{G\omega_n^2}{s^2 + 2\xi\omega_n s + \omega_n^2} \quad 2.30$$

where G is the static gain, ξ is the damping parameter, ω_n is the underdamped natural frequency, and s the Laplace variable ($j\omega$). The inverse transform of equation 2.30 yields the time-domain representation:

$$\hat{H}(t) = \frac{G\omega_n}{\sqrt{1-\xi^2}} e^{-\xi\omega_n t} \sin \omega_n \sqrt{1-\xi^2} t \quad 2.31$$

Comparison of equation 2.28 and 2.31 demonstrates the following relationships which can be used to solve for G , ω_n , and ξ with the known measured parameters of A , B , and ω_d .

$$A = \frac{G\omega_n}{\sqrt{1-\xi^2}} \quad 2.32$$

$$B = \xi\omega_n \quad 2.33$$

$$\omega_d = \omega_n \sqrt{1-\xi^2} \quad 2.34$$

Determination of the stiffness can be made by examining the other common Laplace representation of a second-order system:

$$\hat{H}(s) = \frac{1}{ms^2 + bs + k} \quad 2.35$$

where m is the trunk mass, b is the trunk damping, and k is the trunk stiffness. Comparison of equation 2.35 and 2.30 yields the following relationships to obtain system stiffness, k .

$$m = \frac{1}{G\omega_n^2} \quad 2.36$$

$$b = \frac{2\zeta}{G\omega_n^2} \quad 2.37$$

$$k = \frac{1}{G} \quad 2.38$$

Using this methodology an accurate estimation of trunk stiffness has been made to determine the effects of load level on trunk stiffness during trunk extension exertions²². It is believed that the same procedure can be used to calculate trunk stiffness as a function of varying levels of antagonistic co-activity and load direction

2.4 Reference List

1. Agarwal G.C. and Gottlieb G.L. Compliance of the human ankle joint. J Biomech.Eng. 1977;99:166-70.
2. Baril-Gingras G. and Lortie M. The handling of objects other than boxes: Univariate analysis of handling techniques in a large transport company. Ergonomics 1995;38:905-25.
3. Bendat JS, Piersol AG. Random data: analysis and measurement procedures. 3 ed. New York: John Wiley & Sons, 2000.
4. Bergmark A. Stability of the lumbar spine: A study in mechanical engineering. Acta Orthop.Scand.Suppl. 1989;230:1-54.
5. Chaffin,D.B., Andersson,G.B.J., Martin,B.J. (1999) Occupational Biomechanics, John Wiley and Sons, New York, NY

6. Choi H. Quantitative assessment of co-contraction in cervical musculature. *Med.Eng Phys.* 2003;25:133-40.
7. Cholewicki J. and McGill S.M. EMG assisted optimization: A hybrid approach for estimating muscle forces in an indeterminate biomechanical model. *J.Biomechanics* 1994;27:1287-9.
8. Cholewicki J, Simons APD, and Radebold A. Effects of external trunk loads on lumbar spine stability. *J.Biomechanics* 2000;33:1377-85.
9. Damkot D.K., Pope M.H., Lord J., and Frymoyer J.W. The relationship between work history, work environment and low- back pain in men. *Spine* 1984;9:395-9.
10. Gardner-Morse MG and Stokes IAF. Trunk stiffness increases with steady-state effort. *Journal of Biomechanics* 2001;34:457-63.
11. Granata, K. P. An EMG-Assisted Model of Trunk Loading During Free-Dynamic Lifting. Thesis The Ohio State University 1993
12. Granata KP, Marras WS, and Fathallah FA. A method for measuring external trunk loads during dynamic lifting exertions. *J.Biomechanics* 1995;29:1219-22.
13. Hogan N. Tuning muscle stiffness can simplify control of natural movement. In: Mow V.C., ed. *Advances in Bioengineering*. New York: ASME, 1980:279-82.
14. Hoozemans M.J., van der Beek A.J., Frings-Dresen M.H., van Dijk F.J., and van der Woude L.H. Pushing and pulling in relation to musculoskeletal disorders: a review of risk factors. *Ergonomics* 1998;41:757-81.

15. Hunter I.W. and Kearney R.E. Dynamics of human ankle stiffness: Variation with mean ankle torque. *J.Biomechanics* 1982;15:747-52.
16. Julian F.J. and Morgan D.L. Variations of muscle stiffness with tension during tension transients and constant velocity shortening in the frog. *J.Physiol.* 1981;319:193-203.
17. Kearney RE and Hunter IW. System identification of human stretch reflex dynamics: tibialis anterior. *Exp.Brain Res.* 1984;56:40-9.
18. Kearney RE and Hunter IW. System Identification of Human Joint Dynamics. *Crit.Rev.Biomed.Eng.* 1990;18:55-87.
19. Kerr M, Frank J, Harry S et al. Biomechanical and psychophysical risk factors for low-back pain at work. *Am J.Pub.Health* 2001;91:1069-75.
20. Lee K.S., Chaffin D.B., Herrin G.A., and Waikar A.M. Effect of handle height on lower-back loading in cart pushing and pulling. *Appl.Ergon.* 1991;22:117-23.
21. Marras WS and Mirka GA. A comprehensive evaluation of trunk response to asymmetric trunk motion. *Spine* 1992;17:318-26.
22. Moorhouse KM, Granata K P. Trunk stiffness and dynamics during active extension exertions. In: *J.Biomechanics*. (In Press).
23. Potvin J.R. and Brown A.H.M. Less is more: high pass filtering, to remove up to 99% of the surface EMG signal power, improves EMG-based biceps brachii muscle force estimates. *J. Electr. & Kines.* 2004;14:389-399.

24. Stokes IAF, Gardner-Morse MG, Henry SM, and Badger GJ. Decrease in trunk muscular response to perturbation with preactivation of lumbar spinal musculature. *Spine* 2000;25:1957-64.
25. Vink P., van der Velde E.A., and Verbout A.J. A functional subdivision of the lumbar erector musculature. Recruitment patterns and force-RA-EMG relationships under isometric conditions. *Electromyogr.Clin.Neurophysiol.* 1988;28:517-25.

CHAPTER 3

CO-CONTRACTION RECRUITMENT AND SPINAL LOAD DURING

ISOMETRIC TRUNK FLEXION

Submitted to: *Journal of Biomechanics*

3 January 2005

Kevin P. Granata, Ph.D.

Patrick J. Lee

Timothy C. Franklin

Musculoskeletal Biomechanics Laboratories
Department of Engineering Science & Mechanics
School of Biomedical Engineering & Science
Virginia Polytechnic Institute & State University
219 Norris Hall (0219)
Blacksburg, VA 24061

Address all correspondence to:

K.P. Granata, Ph.D.
Musculoskeletal Biomechanics Laboratories
Department of Engineering Science & Mechanics
Virginia Polytechnic Institute & State University
219 Norris Hall (0219)
Blacksburg, VA 24061
Phone: (540) 231-5316
FAX: (540) 231-4547
Granata@VT.edu

Keywords : Low-Back; Spine; Co-contraction; Push

Abstract

SIGNIFICANCE: Pushing and pulling tasks account for 20% of low-back injury claims in manual materials handling occupation. However, few studies have investigated the neuromuscular recruitment and stabilizing control of the spine during these tasks.

BACKGROUND: The primary torso muscle groups recruited during pushing tasks are the rectus abdominis and the external obliques. However, theoretical analyses suggest that co-contraction of the paraspinal muscles is necessary to stabilize the spine during the flexion exertions. We hypothesize that co-contraction measured during trunk flexion exertions must be greater than co-contraction during extension exertions and that spinal compression during flexion exertions will be greater than during trunk extension exertions of similar trunk moment.

METHODS: Surface EMG was recorded from the trunk muscles of 13 healthy volunteers who maintained isometric trunk posture against horizontal forces applied at the T10 level of the trunk. A biomechanical model was implemented to estimate total muscle force from the measured EMG and trunk moment data. A similar model estimated the muscle forces necessary to achieve equilibrium while minimizing the sum of squared muscle forces. The difference in these forces represented co-contraction. Spinal load attributed to co-contraction was computed from the vector sum of muscle force.

RESULTS: Mean trunk moment was 68.9 Nm and was similar in the flexion and extension exertions. Average co-contraction during flexion exertions was approximately twice the value of co-contraction during extension, i.e. 28% and 13% of total muscle

forces respectively. Co-contraction increased significantly with exertion effort. Co-contraction accounted for up to 47% of the total spinal load during flexion exertions. Consequently, spinal compression during the flexion tasks was nearly 50% greater than during extension exertions despite similar levels of trunk moment.

CONCLUSION: Analyses must consider the role of co-contraction when evaluating spinal load during pushing exertions. Results underscore the need to consider neuromuscular control of spinal stability and recognize the mechanics of multi-segment spine when evaluating the biomechanical risks of trunk flexion and extension exertions.

3.1 Introduction

The primary torso muscle groups recruited for generation of a flexion exertion during pushing tasks are the rectus abdominis and the external obliques. Lumbar paraspinal and posterior internal obliques muscles provide little mechanical potential for the generation of a flexion moment (McGill, 1996). However, if the paraspinal muscles are not recruited during trunk flexion exertions then the spine may become unstable under the loads imposed by the forces from the upper body mass and trunk flexor muscles (Crisco and Panjabi, 1992; Crisco *et al.*, 1992). Hence, antagonistic co-contraction of the lumbar paraspinal muscles during flexion exertions may be necessary to maintain spinal stability (Gardner-Morse *et al.*, 1995; Crisco and Panjabi, 1991). Conversely, during trunk extension exertion such as lifting or pulling tasks the lumbar paraspinal muscles simultaneously generate equilibrium moments and spinal stability (Schultz and Andersson, 1981; Granata and Wilson, 2001). Although co-contraction in the trunk flexor muscles can be recruited to increase stabilizing potential during extension exertion the antagonistic recruitment is typically small (Granata and Orishimo, 2001; Cholewicki *et al.*, 1997). Therefore, less stabilizing co-contraction is expected during trunk extension exertions than during flexion exertions.

The prediction of increased co-contraction during trunk flexion exertions is motivated by the mechanics of spinal equilibrium and stability. Recruitment of flexor muscle activity causes compressive load on the lumbar spine. With the lumbar spine in lordosis the compressive forces at the superior surface of the L5, L4 and L3 vertebrae will cause flexion moment about the base of these spinal units. Muscle forces in the quadratus lumborum and multifidus must be recruited to establish equilibrium about

these vertebrae during flexion exertions. Paraspinal muscle activity during flexion exertions may also be recruited to maintain stability. Stability describes the ability of the musculoskeletal system to maintain equilibrium in the presence of small kinematic or control disturbances. Crisco and Panjabi (1992) illustrated that the lumbar spine is incapable of supporting compressive loads in excess of 88 N without the stabilizing support of paraspinal muscle activation. Spinal compression load during occupational pushing tasks has been estimated at 600 to 1400 N (Schibye *et al.*, 2001). Therefore, muscle recruitment is necessary to support and stabilize the spine during active flexion and extension exertions. Analyses using a one-segment model of the spine indicate that stability of flexion exertions can be achieved by recruiting only flexor muscle activity with minimal co-recruitment of the paraspinal muscle group (Granata and Orishimo, 2001; Cholewicki *et al.*, 1997) if sufficient muscle stiffness and external moment are available. Similarly, extension exertions can be stabilized by recruiting only extensor muscle activity with minimal co-recruitment of the flexor muscles under conditions of sufficient load and muscle stiffness. Conversely, if the stability analyses include a multi-segment model of the spine then flexor muscles alone cannot stabilize the intervertebral segment kinematics (Granata and Wilson, 2001). Engineering control analyses (Appendix 3.6) illustrate that at least one inters-segmental actuator is necessary to achieve controllability of the multi-segment spine. Thus, theoretical analyses agree with previous biomechanical models to suggest that co-contraction during pushing tasks must be greater than during trunk extension exertions (Granata and Bennett, 2004). Empirical measurements of torso muscle co-contraction are necessary to confirm this hypothesis.

Antagonistic co-contraction is operationally defined as muscle recruitment including force components acting in opposition to the desired trunk moment. EMG measurements have quantified lumbar co-contraction during extension exertions but not during flexion exertions (Zetterberg *et al.*, 1987; Marras and Mirka, 1992). Chio (2003) reported co-contraction of the cervical spine muscles by comparing measured muscle forces versus forces minimally necessary to establish equilibrium. Results from that study indicated that co-contraction during cervical flexion exertions accounted for 30% to 40% of the total muscle force whereas co-contraction accounted for 8% to 16% of the total muscle force during extension exertions. Studies of lifting exertions reveal that co-contraction contributes markedly to spinal load (Granata and Marras, 1995b). Therefore, neglect of co-contraction during flexion exertions will result in estimates of spinal load that underestimate actual values (Granata and Bennett, 2004). We are unaware of any study to quantify the difference in co-contraction recruitment during lumbar flexion exertions versus lumbar extension exertions.

The goal of this study was to quantify torso muscle co-contraction and spinal compression during trunk flexion exertions compared with similar data recorded during trunk extension exertions. We hypothesize that co-contraction measured during trunk flexion exertions will be greater than co-contraction during extension exertions. As a result of the co-contraction we also hypothesize that spinal compression during flexion exertions will be greater than during trunk extension exertions of similar moment magnitude. Empirical data were recorded using surface EMG, measured forces and kinematics then inputted into a biomechanical model in order to quantify co-contraction.

3.2 Methods

3.2.1 Experiment

Thirteen healthy volunteers with no history of low back disorders participated in this experiment. Mean (\pm standard deviation) subject mass and stature was 71.4 ± 21.3 kg and 175.1 ± 9.8 cm, respectively. Subjects provided informed consent approved by the Virginia Tech human subjects review board before participation in the experiment.

The protocol required subjects to maintain an upright trunk posture against an external flexion or extension load applied to the trunk. Subjects were secured to a pelvic restraint frame designed to restrict the motion of the pelvis and lower body while in a standing posture (Figure 3.1). A chest harness and cable system attached the subject to a servomotor (Pacific Scientific, Rockford, IL) such that cable tension applied external loads at the T10 level of the trunk. The motor applied isotonic loads of 100, 135, and 170 N. To generate trunk extension exertions the subjects faced the motor such that the cable tension applied a horizontal flexion force. To generate trunk flexion exertions the subjects faced away from the motor such that the cable tension applied a horizontal extension force.

Once subjects confirmed they were at steady state with respect to the applied force, isometric EMG data were recorded. EMG signals were collected using bipolar surface electrodes (Delsys, Boston, MA) on the left and right rectus abdominis (RA), lumbar paraspinals (LP), internal oblique (IO), and external oblique muscles (EO). Briefly, electrodes for the RA were placed 3 cm lateral and 2 cm superior to the umbilicus; LP 4 cm lateral to the L3 spinous process; posterior IO 8 cm lateral to the

midline within the lumbar triangle at a 45^0 ; and EO 10 cm lateral to the umbilicus with an orientation of 45^0 to vertical (Marras and Mirka, 1992). All EMG data were band-pass filtered in hardware between 20 and 500 Hz and sampled at 1000 Hz. The EMG signals were rectified and filtered using a 25 Hz, low-pass, seventh-order Butterworth filter in post-processing software (Matlab, Natick, MA). EMG values from each muscle were normalized with respect to their maximum values recorded during isometric maximum voluntary contraction (MVC) in flexion, extension, right and left lateral twist exertions (McGill, 1991).

Trunk moments were calculated about the L5/S1 joint using inverse dynamic analyses from ground reaction forces as described in Granata et al (Granata *et al.*, 1995). Although subjects maintained an isometric upright trunk posture, 3-D kinematics of the trunk were recorded from electromagnetic sensors (Ascension Technology, Natick MA) taped to the skin over the S1 and T10 vertebrae and at the manubrium (Granata and Sanford, 2000). Processed EMG data, trunk kinetics and kinematics were inputted into a biomechanical model to estimate co-contraction during the flexion and extension exertions.

3.2.2. Biomechanical trunk model

A three-dimensional, two-segment model was implemented to compute muscle force and spinal load (Granata and Wilson, 2001) (Figure 3.2). The two-segment geometry allowed assessment of equilibrium with respect to trunk posture as well as representing intervertebral buckling behavior (Bergmark A., 1989) while retaining simplicity for interpretation of results and assignment of muscle forces. Twelve muscle

equivalents were represented including the right and left RA, EO, IO, and a three component paraspinal muscle on both the right and left sides. The paraspinal muscles included one- and two-segment muscles, e.g. inter-transversus and longissimus thoracic equivalent muscles. Anthropometric origin, insertion and cross-sectional area of each muscle were established from published anatomy (Jorgensen *et al.*, 2001; Marras W.S. *et al.*, 2001) and described elsewhere (Granata and Wilson, 2001). The moment generating capacity of each muscle was determined from the vector product between the unit vector direction of muscle force, \hat{F}_i , and the muscle origin, r_i , for each muscle $i=1..12$. This was scaled by the muscle force magnitude, F_i , to determine muscle moment. The sum of muscle moments must achieve equilibrium with respect to the measured external moments (equation 3.1).

$$M_{ext} = \sum_{i=1}^n F_i \{r_i \times \hat{F}_i\} \quad n = 12 \quad (3.1)$$

$$F_i = \text{Gain} \alpha_i \text{Area}_i f(\text{Len}_i) f(\text{Vel}_i) \quad i=1..12 \quad (3.2)$$

$$0 \leq \alpha_i \leq 1 \quad (3.3)$$

Magnitude of force in each muscle (equation 3.2) was determined from the product of muscle activation, α_i , muscle cross-sectional area, Area_i , muscle Gain, and modulating factors to represent physiologic effects of force-length, $f(\text{Len}_i)$, and force-velocity, $f(\text{Vel}_i)$ as described in our previous spine models (Granata and Marras, 1995a). Recognizing that the exertions represented an isometric upright posture, the force-length and force-velocity values were set to unity. Gain represented force capacity per unit cross-sectional area of the muscles and were calibrated for each subject. To be physiological valid the

predicted Gain values must lie between 30 and 100 N cm⁻² (Reid *et al.*, 1912; McGill and Norman, 1986).

Co-contraction was determined from muscle forces by solving for activations, α_i , from measured EMG and comparing them with the values necessary for equilibrium. In the EMG-assisted approach equilibrium was achieved by determining the Gain value necessary to satisfy equations 1 and 2 with constraints requiring that α_i must be equal to normalized EMG_{*i*} for each muscle $i = 1..12$. Activation values of the three components of the LP muscle were equally distributed and numerically equivalent to the normalized EMG recorded from the LP electrode site. Note that muscle forces determined from this EMG-assisted approach includes components necessary to achieve equilibrium plus the effects of co-contraction, F_{i_Total} . The set of muscle forces necessary to achieve equilibrium without co-contraction, F_{i_Equil} , were estimated by means of linear programming. Specifically, the set of α_i were determined to minimize the sum of squared muscle force with equilibrium equality constraint (equation 3.1) and activation boundary constraints (equation 3.3). The Gain contributes to the force magnitude determined from this analysis and was therefore calibrated prior to estimation of α_i by setting it equal to the Gain value computed from the EMG-assisted model described above. As per the methods of Choi (2003) the components of muscle force attributed to co-contraction were determined by comparing the muscle forces from these two analyses,

$$F_{i_Co-Contr} = F_{i_Total} - F_{i_Equil} \quad (3.4)$$

Co-contraction was expressed as the percentage of total muscle force attributed to co-contraction, i.e. the ratio of the sum of $F_{i_Co-Contr}$ versus the sum of F_{i_Total} .

$$Co-contraction = 100 \left\{ \frac{\sum_{i=1}^n F_{i\ Co-Contr}}{\sum_{i=1}^n F_{i\ Total}} \right\} \quad (3.5)$$

Spinal load was computed as the vector sum of muscle forces and included components of spinal compression attributed to co-contraction and spinal compression attributed to equilibrium muscle forces.

Statistical analyses were performed to determine the effects of flexion versus extension and exertion level (100 N, 135 N, 170 N). A two factor (flexion/extension, exertion level) repeated measures ANOVA were performed with dependent variables including co-contraction and spinal compression. Analyses were performed using commercial software (Statistica, 4.5 Statsoft, Inc., Tulsa OK) with a significance level of $\alpha < 0.05$. Tukey honest-significant difference (HSD) post-hoc analyses were used to compare differences among significant treatments.

3.3 Results

Predicted values of the muscle gains provided insight to the performance of the model. The average gain was 47.5 ± 21.3 N/cm² and well within the physiological accepted range of 30 to 100 N/cm². The errors between predicted and experimentally measured moments were small, i.e. average error 1.2% during flexion and 2.1% during extension exertions. Mean trunk moment was 68.9 ± 10.9 Nm. The experimental protocol applied similar horizontal external forces to the trunk during both flexion and extension exertions, so it is not surprising that trunk moments were not significantly ($p < 0.412$) different in flexion and extension exertions. Trunk moment increased

significantly ($p < 0.05$) with exertion level from 59.3 ± 6.8 Nm during 100 N load conditions to 80.8 ± 5.2 Nm during conditions at 170 N loads.

Results demonstrated that the co-contraction ratio was significantly ($p < 0.01$) greater during flexion exertions than during extension exertions. The average co-contraction during flexion was approximately twice the value during extension, $27.9 \pm 10.4\%$ and $13.3 \pm 5.8\%$ respectively. Co-contraction increased significantly ($p < 0.01$) with respect to exertion level, ranging from mean levels of $12.1 \pm 8.0\%$ at 100 N load to $30.9 \pm 9.3\%$ during conditions at 170 N load. There was no significant interaction between exertion level and flexion/extension ($p = 0.783$).

Recognizing that co-contraction was greater during flexion exertions than during extension despite similar trunk moments, one must expect differences in spinal load attributed to the muscle forces. During flexion exertions the spinal compression was significantly ($p < 0.05$) greater than during extension exertions. Average spinal compression during flexion was 1520.7 ± 250.3 N while the average spinal compression during extension was 1037 ± 172.1 N. Spinal compression increased significantly ($p < 0.05$) with respect to exertion level, from a mean value of 835 ± 89 N during 100 N load conditions to 1736 ± 289 N during 170 N load conditions. Recall that the force in each muscle included components necessary to achieve the task equilibrium, F_{Equil} , plus the force attributed to muscle co-contraction, $F_{\text{Co-contr}}$. The compressive load attributed to the equilibrium components of muscle force, F_{Equil} , was not significantly ($p = 0.312$) influenced by flexion/extension. Compressive load attributed to co-contraction, $F_{\text{Co-contr}}$, was significantly ($p < 0.01$) greater during flexion exertions than during extension exertions. $F_{\text{Co-contr}}$ ($p < 0.01$) contributed to increased spinal compression with increased

exertion level. Thus, co-contraction significantly affected spinal loads during both flexion and extension exertions.

3.4 Discussion

Pushing and pulling tasks account for 20% of low-back injury claims in manual materials handling occupations (Damkot *et al.*, 1984). However, few studies have investigated the neuromuscular recruitment and stabilizing control of the spine during these tasks (McGill, 1996). The primary torso muscle groups recruited for generation of a flexion exertion during pushing tasks are the rectus abdominis and the external obliques (Lee *et al.*, 1989; Andres and Chaffin, 1991). However, if the paraspinal muscles are not recruited during trunk flexion exertions then the spine may become unstable under the loads imposed by the upper body mass and trunk flexor muscle forces (Crisco and Panjabi, 1992; Crisco *et al.*, 1992; Kiefer A. *et al.*, 1998). Engineering control systems analyses (Appendix) of a multi-segment representation of the spinal column illustrates that inter-segmental actuators are necessary to achieve stabilizing control of the spine during flexion exertions. Interpretation of this analysis suggests that paraspinal muscle recruitment is necessary during flexion exertions despite the fact these muscles are antagonistic to the flexion exertion. Biomechanical analyses of applied forces and trunk postures during pushing tasks similarly concluded that stabilizing co-contraction should be expected (Granata and Bennett, 2004). Although co-contraction during trunk extension exertions may be recruited to augment stability during trunk extension exertions (Granata and Orishimo, 2001) the theoretical analyses indicate that co-

contraction must be greater during flexion exertions than during trunk extension exertions.

Co-contraction during trunk flexion exertions was approximately twice the level of co-contraction during equivalent extension tasks. Co-contraction was computed by comparing muscle forces from a published EMG-assisted model of the spine mechanics (Granata and Wilson, 2001) versus muscle forces estimated from a similar model that predicted the recruitment necessary to achieve equilibrium. Note that muscles forces determined from EMG-assisted models include the effects of co-contraction (Granata and Marras, 1995b). Muscle recruitment determined by methods of optimization are capable of predicting equilibrium muscle forces but overlook co-contraction (Collins J.J., 1995). Therefore, the difference between these results can be used as an estimate of co-contraction. Results represent co-contraction of the lumbar musculature but agree with similar analyses of the musculature surrounding the cervical spine (Choi, 2003). In the current study the mean co-contraction was approximately 28% and 13% of the total muscle force during flexion and extension exertions respectively whereas Choi (2003) reported mean values of 35% and 12% for the cervical spine. Thus, relative trends agree with published values while differences in absolute values might be explained by anthropometric differences between the lumbar and thoracic spine.

Why compute co-contraction using a biomechanical model instead of direct comparison of EMG data between flexion and extension exertions? When recording EMG activity during voluntary exertions the coactivity in antagonistic muscles can be determined by a priori characterization of muscle function (Granata *et al.*, 2001; Granata and Orishimo, 2001). However, when comparing results between different tasks and

moment directions, one must account for the fact that most muscles generate moments about more than one anatomic axis. Therefore, biomechanical analyses are required to characterize muscle function as agonist, antagonist, and equipoise (Hughes *et al.*, 1994). Moreover, when estimating trunk moment from EMG activity of rectus abdominis versus moment from EMG in the paraspinal muscles, one must consider the relative moment arm and size of these muscle groups with respect to the respective flexion and extension exertions. Thus, it is reasonable to quantify co-contraction by means of a biomechanical model in order to gain insight into the role of neuromuscular recruitment during pushing, pulling and lifting tasks (Marras W.S. and Granata K.P., 1997). Moreover, the assessments provide insight into the neuromuscular factors that contribute to spinal load during these exertions.

Co-contraction contributes to spinal load but has been largely overlooked in analyses of pushing tasks. Estimates of spinal load that neglect co-contraction may underestimate compression by as much as 45% during lifting tasks (Granata and Marras, 1995b). Nonetheless, estimates of spinal load during pushing tasks often neglect co-contraction. Chaffin and colleagues implemented a single-equivalent muscle model to estimate spinal loads associated with workplace pushing tasks (Lee *et al.*, 1989; Resnick M.L. and Chaffin D.B., 1995; Andres and Chaffin, 1991). Similar models were employed by Kumar (1994) and DeLooze (1995) whereas Schibye (2001) employed the Watback regression analyses to estimate spinal load. Discussing their model of pushing, Lee (1989) noted that the “solution assumes that only one muscle at a time is active to stabilize the torso (i.e. no antagonism exists)” and that single equivalent models that ignore co-contraction “may not be appropriate for the estimation of muscle forces in the

lower back.” Results from the current study illustrate that up to 46.7% of the spinal load during flexion exertions are attributable to co-contraction. Consequently, spinal compression during the flexion tasks was nearly 50% greater than during extension exertions. This is in contrast to published studies that report less spinal compression during pushing tasks than typically observed in lifting exertions (Schibye *et al.*, 2001; deLooze M.P. *et al.*, 1995). In those studies the reduction in spinal load was attributed the fact that trunk moment magnitude during pushing tasks were small when compared to lifting tasks. The protocol described in the current study examined flexion and extension exertions with similar trunk moment magnitude. Therefore, we conclude that co-contraction and associated spinal load during flexion exertions is greater than during similar trunk extension exertions. However, further analyses are necessary to investigate the role of co-contraction during simulated workplace tasks involving pushing and pulling.

Co-contraction and spinal load increased with exertion level. It has been well established that primary agonist muscle activation, muscle force and spinal load increase with trunk moment (Schultz and Andersson, 1981). This effect of task load was evident in the results wherein the spinal load attributable to equilibrium specific muscle forces, F_{Equil} , increased significantly with exertion level. However, co-contraction also increased with exertion effort in both flexion and extension. During 100 N load conditions the mean co-contraction was 12% of the total muscle force whereas during 170 N load conditions the co-contraction was nearly 31% of the total muscle force. This effect can be explained in part by equilibrium requirements. Spinal compression from flexor muscle activity causes moments about the L5, L4 and L3 vertebrae that requiring

paraspinal recruitment to establish equilibrium. Hence, increased flexor force requires greater LP co-contraction. Unfortunately, this does not fully explain this effect because similar observations were reported in measures of EMG coactivity that increase with lumbar extension moment (Marras W.S. and Mirka, 1993; Song and Chung, 2004). Recent biomechanical analyses illustrate that co-contraction recruitment can be explained in part by spinal stability requirements (Granata and Orishimo, 2001; Cholewicki *et al.*, 1997). Those theoretical stability analyses predict that antagonistic co-contraction should decline with increased trunk moment but published empirical measurements of stability document increased co-contraction with external load (Granata and Orishimo, 2001). To describe this stabilizing control behavior nonlinear controllability models must be implemented. Although further research is necessary to understand this behavior the results are consistent with published data but. Results suggest that analyses of workplace pushing and pulling exertions must consider the role of exertion effort on the co-contraction contributions to spinal load.

Further research is necessary to quantify the stability of the spine. During extension tasks the muscle recruitment directly contributes to spinal stability. During flexion tasks augmented recruitment patterns are necessary to maintain spinal stability. Results may indicate greater risk of spinal instability from motor control error during trunk flexion tasks than during extension exertions (Granata and Bennett, 2004). However, data in this study did not quantify spinal stability. Although insight can be achieved from motor control assessments of seated balance (Cholewicki *et al.*, 2000) there are no existing quantitative measures of spinal stability. To understand neuromuscular risk of low-back injury it will be necessary to develop quantitative

assessments of spinal stability. Moreover, the analyses described here represent static exertions. Further research is necessary to quantify the role of dynamic flexion tasks on muscle recruitment, spinal load and stability.

In conclusion, co-contraction during isometric lumbar flexion exertions is greater than during extension exertions. This has been attributed to spinal stability requirements. Results underscore the need to consider neuromuscular control of spinal stability when evaluating the biomechanical risks of trunk flexion and extension exertions.

3.5 Acknowledgement

This research was supported in part by a grant R01 AR49932 from CDC / National Institute for Occupational Safety and Health. We wish to thank G. Slota for his assistance in the analysis and interpretation of the data.

3.6 Appendix

Controllability analyses can be used to determine whether specified actuators, f_i , can successfully stabilize and control the associated system. A two-dimensional model of the spine included four muscle actuators representing three muscle slips of the lumbar paraspinal muscles, f_1 , f_2 , f_3 , and a fourth actuator representing the rectus abdominis, f_4 (Figure 2). Muscle origins and insertions were assigned to vector locations p_i and d_i respectively for muscles f_i , where $i=1..4$. The spine was represented as two-segment inverted pendulum. The controllability analysis was limited to a sagittal plane representation of dynamics whereas the biomechanical model for co-contraction (see Methods) employed three-dimensional analyses. The controllability analysis also ignored the internal oblique and external oblique muscles. However, the system can be expanded to demonstrate similar results if these muscle groups are included in a 3-D model.

System dynamics were determined by Lagrange analyses with arbitrary values of segment mass, m_1 and m_2 , and center of mass. The torso mass was included with the mass and center of mass of the second (upper) segment. The equations of dynamics result in a set of two simultaneous equations of motion including segment angle, θ_1 , θ_2 , angular velocity, $\dot{\theta}_1$, $\dot{\theta}_2$, and angular acceleration $\ddot{\theta}_1$, $\ddot{\theta}_2$.

$$\mathbf{M}(\theta_1, \theta_2) \cdot \begin{Bmatrix} \ddot{\theta}_1 \\ \ddot{\theta}_2 \end{Bmatrix} + \mathbf{C}(\theta_1, \theta_2) \cdot \begin{Bmatrix} \dot{\theta}_1^2 \\ \dot{\theta}_2^2 \end{Bmatrix} + \mathbf{F}_{Ext}(\theta_1, \theta_2) + \mathbf{G}(\theta_1, \theta_2) = \begin{Bmatrix} \mathbf{Q}_{\theta 1} \\ \mathbf{Q}_{\theta 2} \end{Bmatrix} \quad (\text{A1})$$

$$\begin{Bmatrix} Q_{\theta 1} \\ Q_{\theta 2} \end{Bmatrix} = \mathbf{Q}(\theta_1, \theta_2) \cdot \bar{\mathbf{f}} \quad (\text{A2})$$

$\mathbf{M}(\theta_1, \theta_2)$ represents a 2-by-2 matrix of inertia that was is a function of equilibrium geometry, θ_1, θ_2 . Bold characters represent matrices. Values $\mathbf{C}(\theta_1, \theta_2)$, $\mathbf{F}_{\text{Ext}}(\theta_1, \theta_2)$ and $\mathbf{G}(\theta_1, \theta_2)$ represented the 2-by-2 matrix of velocity coefficients, the 2-by-1 external force vector, and the 2-by-1 gravity vector. Actuation torques $\mathbf{Q}_{\theta_1}(\theta_j, f_i)$ and $\mathbf{Q}_{\theta_2}(\theta_j, f_i)$ were expressed as a product of the moment-arm matrix $\mathbf{Q}(\theta_1, \theta_2)$ and the vector of actuator (muscle) forces, $\bar{\mathbf{f}} = [f_1 \ f_2 \ f_3 \ f_4]^T$.

The second-order equations of dynamics were linearized about the equilibrium posture, θ_1, θ_2 , and expressed as a first-order state space equation (A3) with respect to the state vector $\bar{\mathbf{x}} = \{\theta_1, \dot{\theta}_1, \theta_2, \dot{\theta}_2\}$. This state-space representation included actuation forces, $\bar{\mathbf{f}} = \bar{\mathbf{f}}_o + \bar{\mathbf{f}}_k$, with components of both equilibrium forces, f_0 and perturbation forces, f_k .

$$\dot{\bar{\mathbf{x}}} = \mathbf{A} \cdot \bar{\mathbf{x}} + \bar{\mathbf{F}} + \mathbf{B} \cdot \bar{\mathbf{f}} \quad (\text{A3})$$

where $\mathbf{A} = -\mathbf{M}^{-1} \cdot \mathbf{G}$ and $\mathbf{B} = \mathbf{M}^{-1} \cdot \mathbf{Q}$ are 4-by-4 matrices. The linearization process eliminated the velocity coefficient matrix $\mathbf{C}(\theta_1, \theta_2)$, and reveals an equilibrium constant $\bar{\mathbf{F}} = -\mathbf{M}^{-1} \cdot (\mathbf{F}_{\text{Ext}})$ that must be balanced by the actuation equilibrium moment, i.e. $\mathbf{B} \cdot \bar{\mathbf{f}}_o = -\bar{\mathbf{F}}$.

The system is controllable if $\text{Rank}(\mathbf{Cm}) = 4$, where \mathbf{Cm} is known as the controllability matrix $\mathbf{Cm} = [\mathbf{B}, \mathbf{A} \cdot \mathbf{B}, \mathbf{A}^2 \cdot \mathbf{B}, \mathbf{A}^3 \cdot \mathbf{B}]$. No assumptions regarding muscle models were required other than the fact that muscles can generate force and that the muscles can establish equilibrium. If one assumes the perturbation forces, f_k , is

proportional to the system state, \bar{x} , i.e. muscle force due to stiffness and damping,

$\bar{f}_k = \mathbf{K} \cdot \bar{x}$, then the dynamic response about the equilibrium state can be expressed as

$$\dot{\bar{x}} = [\mathbf{A} + \mathbf{B} \cdot \mathbf{K}] \cdot \bar{x} \quad (\text{A4})$$

The system is stable if the real component of all eigenvalues of $[\mathbf{A} + \mathbf{B} \cdot \mathbf{K}]$ are less than zero. Three cases of control behavior will be evaluated.

Case 1: Flexion exertion utilizing only abdominal muscle group f_4

$$\mathbf{A} = \begin{bmatrix} 0 & 1 & 0 & 0 \\ \frac{2g(m_1 + 2 \cdot m_2)}{L1 \cdot m_1} & 0 & -\frac{4g \cdot m_2}{L1 \cdot m1} & 0 \\ 0 & 0 & 0 & 1 \\ \frac{4g(m_1 + 2 \cdot m_2)}{L2 \cdot m_1} & 0 & \frac{2g(m_1 + 2 \cdot m_2)}{L2 \cdot m_1} & 0 \end{bmatrix}, \quad \mathbf{B} = \begin{bmatrix} 0 & 0 & 0 & 0 \\ 0 & 0 & 0 & B_{24} \\ 0 & 0 & 0 & 0 \\ 0 & 0 & 0 & B_{44} \end{bmatrix} \quad (\text{A5})$$

where g is the gravitational constant, $g=9.8$ m/sec. Note that the first three columns of \mathbf{B} are zero. This represents the condition wherein the paraspinal muscles, f_1 , f_2 , and f_3 are zero. \mathbf{B} has been represented symbolically as its entries are long and complicated.

Nonetheless, from the form of these matrices it is clear that $\text{Rank}(\mathbf{Cm}) \leq 2$. Therefore, this system is not controllable and subsequently not stabilizable. Hence, without paraspinal muscle co-contraction multi-segment spine cannot be stabilized during a flexion exertion.

Case 2: Flexion exertion utilizing abdominal muscle group f_4 and lumbar paraspinal muscles f_1 . The \mathbf{A} matrix is identical to case 1 above, but the \mathbf{B} matrix includes nonzero elements in column 1 to permit actuation of f_1 .

$$\mathbf{B} = \begin{bmatrix} 0 & 0 & 0 & 0 \\ B_{21} & 0 & 0 & B_{24} \\ 0 & 0 & 0 & 0 \\ B_{41} & 0 & 0 & B_{44} \end{bmatrix} \quad (\text{A6})$$

For physiological values, $\text{Rank}(\mathbf{Cm}) = 4$ thereby demonstrating that the system is controllable only if antagonistic muscle co-contraction in the paraspinal muscles are recruited.

Case 3: Extension exertion utilizing paraspinal muscle groups f_1 and f_2 with no abdominal muscle activation. The \mathbf{A} matrix is identical to case 1 above, but the \mathbf{B} matrix includes nonzero elements in columns 1 and 2 to permit actuation of f_1 and f_2

$$\mathbf{B} = \begin{bmatrix} 0 & 0 & 0 & 0 \\ B_{21} & B_{22} & 0 & 0 \\ 0 & 0 & 0 & 0 \\ B_{41} & B_{42} & 0 & 0 \end{bmatrix} \quad (\text{A7})$$

For physiological values $\text{Rank}(\mathbf{Cm}) = 4$, thereby demonstrating that the system is controllable despite the fact that co-contraction of the flexor muscles is prohibited in this scenario. Optimized actuator performance can be achieved by permitting recruitment of f_3 . However, to be stable the eigenvalues of $[\mathbf{A} + \mathbf{B} \cdot \mathbf{K}]$ must be less than zero, thereby requiring sufficiently large values of \mathbf{K} . With the implementation of a muscle model, it is possible to increase muscle stiffness by increasing muscle force; thus, the above \mathbf{K} found for stability can be achieved through increasing muscle force. In order to maintain the equilibrium posture antagonist groups must also activate to balance this increase in extensor moment. Previous analyses (Granata and Orishimo, 2001; Cholewicki *et al.*,

1997; Gardner-Morse and Stokes, 1998) illustrate that if \mathbf{K} is insufficiently large, then antagonistic co-contraction in the flexor muscles can be used to augment the extensor muscle stiffness and contribute to the system stability. Therefore, co-contraction during trunk extension exertions may be recruited to augment stability. Conversely, co-contraction during trunk flexion exertions must be recruited for stability.

This analysis requires perturbation muscle forces, f_k , that can achieve both positive and negative values with respect to equilibrium force f_0 . In so far as f_0 is greater than zero, this criteria is physiologically valid. Specifically, the biomechanical impedance of active muscle permits the muscle force to become greater than the equilibrium force value when stretched or to be less than the baseline equilibrium force when shortened. Although these analyses demonstrate controllability, if one wishes to accurately predict specific values of active muscle force and co-contraction then nonlinear muscle models and nonlinear control analyses must be implemented. Nonetheless, the analyses demonstrate that co-contraction is necessary during trunk flexion exertions and suggests the co-contraction during flexion exertions must be greater than co-contraction during extension exertions.

3.7 References

- Andres, R.O. and Chaffin, D.B. (1991) Validation of a biodynamic model of pushing and pulling. *J. Biomechanics* **24**, 1033-1045.
- Bergmark A. (1989) Stability of the lumbar spine: A study in mechanical engineering. *Acta Orthop. Scand. Suppl.* **230**, 1-54.
- Choi, H. (2003) Quantitative assessment of co-contraction in cervical musculature. *Med. Eng. Phys.* **25**, 133-140.

- Cholewicki,J., Panjabi,M.M., and Khachatryan,A. (1997) Stabilizing function of trunk flexor-extensor muscles around a neutral spine posture. *Spine* **22**, 2207-2212.
- Cholewicki,J., Polzhofer,G.A., and Radebold,A. (2000) Postural control of trunk during unstable sitting. *J.Biomechanics* **22**, 1733-1737.
- Collins J.J. (1995) The redundant nature of locomotor optimization laws. *J.Biomechanics* **28**, 251-267.
- Crisco,J.J. and Panjabi,M.M. (1991) The intersegmental and multisegmental muscles of the lumbar spine: A biomechanical model comparing lateral stabilizing potential. *Spine* **16**, 793-799.
- Crisco,J.J. and Panjabi,M.M. (1992) Euler stability of the human ligamentous lumbar spine: Part I Theory. *Clin.Biomech.* **7**, 19-26.
- Crisco,J.J., Panjabi,M.M., Yamamoto,I., and Oxland,T.R. (1992) Euler stability of the human ligamentous lumbar spine. Part II Experiment. *Clin.Biomech.* **7**, 27-32.
- Damkot,D.K., Pope,M.H., Lord,J., and Frymoyer,J.W. (1984) The relationship between work history, work environment and low- back pain in men. *Spine* **9**, 395-399.
- deLooze M.P., Stassen A.R.A., Markslag A.M.T., Borst M.J., Wooning M.M., and Toussaint H.M. (1995) Mechanical loading of the low back in three methods of refuse collecting. *Ergonomics* **38**, 1993-2006.
- Gardner-Morse,M.G. and Stokes,I.A.F. (1998) The effects of abdominal muscle coactivation on lumbar spine stability. *Spine* **23**, 86-92.
- Gardner-Morse,M.G., Stokes,I.A.F., and Laible,J.P. (1995) Role of muscles in lumbar stability in maximum extension efforts. *J.Orthop.Res.* **13**, 802-808.
- Granata,K.P. and Bennett,B.E. Low-back biomechanics and stability during pushing. Hum.Factors . 2004.
Ref Type: In Press
- Granata,K.P. and Marras,W.S. (1995a) An EMG assisted model of biomechanical trunk loading during free-dynamic lifting. *J.Biomechanics* **28**, 1309-1317.
- Granata,K.P. and Marras,W.S. (1995b) The influence of trunk muscle coactivity upon dynamic spinal loads. *Spine* **20**, 913-919.
- Granata,K.P., Marras,W.S., and Fathallah,F.A. (1995) A method for measuring external trunk loads during dynamic lifting exertions. *J.Biomechanics* **29**, 1219-1222.
- Granata,K.P. and Orishimo,K. (2001) Response of Trunk Muscle Coactivation to Changes in Spinal Stability. *J.Biomechanics* **34**, 1117-1123.

- Granata,K.P., Orishimo,K., and Sanford,A.H. (2001) Trunk Muscle Coactivation in Preparation for Sudden Load. *J.Electromyo.Kinesiol.* **11**, 247-254.
- Granata,K.P. and Sanford,A.H. (2000) Lumbar-pelvic coordination is influenced by lifting velocity and task weight. *Spine* **25**, 1413-1418.
- Granata,K.P. and Wilson,S.E. (2001) Trunk Posture and Spinal Stability. *J.Biomechanics* **16**, 650-659.
- Hughes,R.E., Chaffin,D.B., Lavender,S.A., and Andersson,G.B. (1994) Evaluation of muscle force prediction models of the lumbar trunk using surface electromyography. *J.Orthop.Res.* **12**, 689-698.
- Jorgensen,M.J., Marras,W.S., Granata,K.P., and Wiand,J.W. (2001) MRI-derived moment-arms of the female and male spinal loading muscles. *Clin.Biomech.* **16**, 182-193.
- Kiefer A., Shirazi-Adl A., and Parnianpour M. (1998) Synergy of the human spine in neutral postures. *Eur.Spine J.* **7**, 471-479.
- Kumar S. (1994) The back compressive forces during maximal push-pull activities in the sagittal plane. *J.Human.Ergol.* **23**, 133-150.
- Lee,K.S., Chaffin,D.B., Waikar,A.M., and Chung,M.K. (1989) Lower back muscle forces in pushing and pulling. *Ergonomics* **32**, 1552-1563.
- Marras W.S. and Granata K.P. (1997) The development of an EMG-assisted model to assess spine loading during whole-body free-dynamic lifting. *J.Electromyo.Kinesiol.* **7**, 259-268.
- Marras W.S., Jorgenson M.J., Granata K.P., and Wiand B (2001) Female and male trunk geometry: Size and prediction of the spine loading trunk muscles derived from MRI. *Clin.Biomech.* **16**, 38-46.
- Marras W.S. and Mirka,G.A. (1993) Electromyographic studies of the lumbar trunk musculature during the generation of low-level trunk acceleration. *Mirka G.A.* **11**, 811-817.
- Marras,W.S. and Mirka,G.A. (1992) A comprehensive evaluation of trunk response to asymmetric trunk motion. *Spine* **17**, 318-326.
- McGill,S.M. (1991) Electromyographic activity of the abdominal and low back musculature during the generation of isometric and dynamic axial trunk torque: Implications for lumbar mechanics. *J.Orthop.Res.*; **9**, 91-103.
- McGill,S.M. (1996) A revised anatomical model of the abdominal musculature for torso flexion efforts. *J.Biomechanics* **29**, 973-977.

McGill,S.M. and Norman,R.W. (1986) Partitioning the L4-L5 dynamic moment into disc, ligamentous, and muscular components during lifting. *Spine* **11**, 666-678.

Reid,J.G., Costigan,P.A., and Comrie,W. (1912) Prediction of trunk muscle areas and moment arms by use of anthropometric measures. *Spine* **3**, 273-275.

Resnick M.L. and Chaffin D.B. (1995) An ergonomic evaluation of handle height and load in maximal and submaximal cart pushing. *Appl.Ergon.* **26**, 173-178.

Schibye,B., Sogaard,K., Martinsen,D., and Klausen,K. (2001) Mechanical load on the low back and shoulders during pushing and pulling of two-wheeled waste containers compared with lifting and carrying of bags and bins. *Clin.Biomech.* **16**, 549-559.

Schultz,A.B. and Andersson,G.B. (1981) Analysis of loads on the lumbar spine. *Spine* **6**, 76-82.

Song,Y.W. and Chung,M.K. (2004) Quantitative assessment of trunk muscle coactivation in sub-maximal isometric exertion tasks. *International Journal of Industrial Ergonomics* **34**, 13-20.

Zetterberg,C., Andersson,G.B., and Schultz,A.B. (1987) The activity of individual trunk muscles during heavy physical loading. *Spine* **12**, 1035-1040.

3.8 Figures and Tables

Figure 3.1. Experimental setup. The external load acts anteriorly on the subject during an extension exertion trial in position shown. During a flexion exertion trial the subject was rotated 180° from the shown position so the external load acted posteriorly on the subject. EMG data were collected on four muscle groups at steady-state preload. Subjects were securely strapped into a rigid pelvic support structure to isolate movement of the trunk for all trials.

Figure 3.2. Schematic representation of trunk musculature used to quantify trunk co-contraction during trunk flexion and extension. For clarity, the external obliques and internal obliques muscles have been omitted but were included in the computational analysis.

Figure 3.3. Co-contraction levels were significantly greater during flexion exertions ($p < 0.01$). Co-contraction levels were significantly greater with respect to load ($p < 0.01$). There was no significant interaction between load direction and load ($p = 0.783$).

Table 3.1. Model predicted spinal compression (N) from total muscle forces, task muscle forces, and co-contraction during all three load levels. The effect of load level ($p > 0.05$) and load direction ($p > 0.05$) were both statistically significant on spinal compression. Measured moment were not significantly ($p < 0.712$) with respect to load direction. Measured moment was significantly ($p < 0.05$) different with respect to load level.

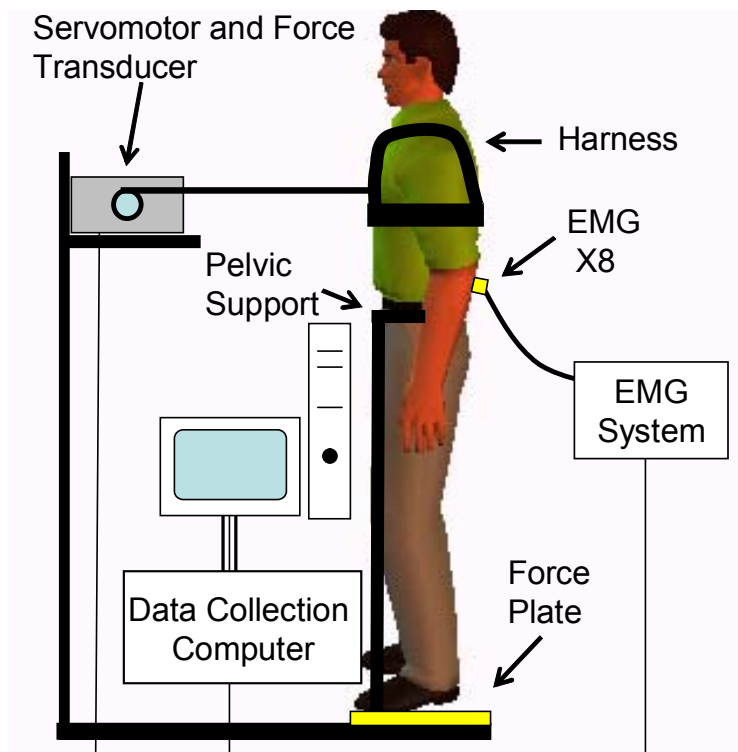


Figure 3.1. Experimental setup. The external load acts anteriorly on the subject during an extension exertion trial in position shown. During a flexion exertion trial the subject was rotated 180° from the shown position so the external load acted posteriorly on the subject. EMG data were collected on four muscle groups at steady-state preload. Subjects were securely strapped into a rigid pelvic support structure to isolate movement of the trunk for all trials.

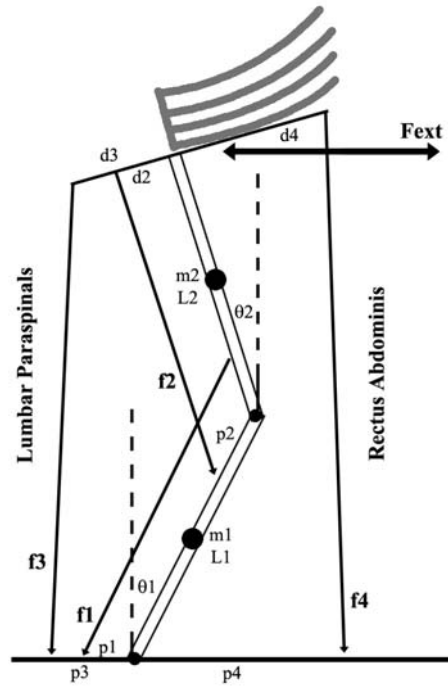


Figure 3.2. Schematic representation of trunk musculature used to quantify trunk co-contraction during trunk flexion and extension. For clarity, the external obliques and internal obliques muscles have been omitted but were included in the computational analysis.

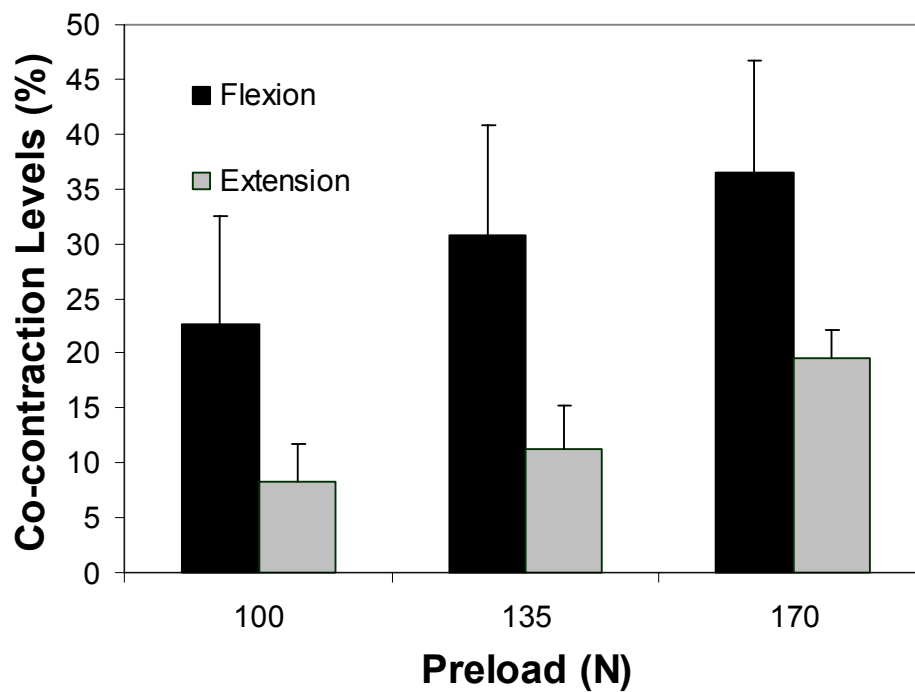


Figure 3.3. Co-contraction levels were significantly greater during flexion exertions ($p < 0.01$). Co-contraction levels were significantly greater with respect to load ($p < 0.01$). There was no significant interaction between load direction and load ($p = 0.783$).

Table 3.1. Model predicted spinal compression (N) from total muscle forces, task muscle forces, and co-contraction during all three load levels. The effect of load level ($p > 0.05$) and load direction ($p > 0.05$) were both statistically significant on spinal compression. Measured moment were not significantly ($p < 0.712$) with respect to load direction. Measured moment was significantly ($p < 0.05$) different with respect to load level

	Load Level (N)		
	100	135	170
<i>Spinal Compression (N)</i>			
Flexion			
Compression from total muscle force	995 ± 162	1501 ± 215	2066 ± 352
Compression from task muscle force	769.6 ± 75	1039.8 ± 95	1312 ± 165
Compression from co-contraction	225.4 ± 98	461.2 ± 151	754 ± 210
Extension			
Compression from total muscle force	675 ± 108	1028 ± 165	1407 ± 230
Compression from task muscle force	619.1 ± 99	912.8 ± 153	1131.4 ± 270
Compression from co-contraction	55.9 ± 23	115.2 ± 41	275.6 ± 37
<i>Measured Moment (Nm)</i>			
Flexion	57.3 ± 4.3	68.9 ± 5.2	82.3 ± 9.5
Extension	55.1 ± 5.4	70.9 ± 6.3	79.21 ± 9.1

CHAPTER 4

ACTIVE TRUNK STIFFNESS INCREASES WITH CO-CONTRACTION

Submitted to: *Journal of Electromyography and Kinesiology*

21 December 2004

Patrick J. Lee

Ellen L. Rogers

Kevin P. Granata, Ph.D.

Musculoskeletal Biomechanics Laboratories
Department of Engineering Science & Mechanics
School of Biomedical Engineering & Science
Virginia Polytechnic Institute & State University
219 Norris Hall (0219)
Blacksburg, VA 24061

Address all correspondence to: K.P. Granata, Ph.D.
Musculoskeletal Biomechanics Laboratories
Department of Engineering Science & Mechanics
Virginia Polytechnic Institute & State University
219 Norris Hall (0219)
Blacksburg, VA 24061
Phone: (540) 231-5316
FAX: (540) 231-4547
Granata@VT.edu

KEYWORDS : Co-activation, Spine, Stiffness

Abstract

Trunk dynamics, including stiffness, mass and damping were quantified during trunk extension exertions with and without voluntary recruitment of antagonistic co-contraction. The objective of this study was to empirically evaluate the influence of co-activation on trunk stiffness. Muscle activity associated with voluntary co-contraction has been shown to increase joint stiffness in the ankle and elbow. Although biomechanical models assume coactive recruitment causes increase trunk stiffness it has never been empirically demonstrated. Small trunk displacements invoked by pseudorandom force disturbances during trunk extension exertions were recorded from seventeen subjects at two co-contraction conditions (minimal and maximal voluntary co-contraction recruitment). EMG data were recorded from eight trunk muscles as a baseline measure of co-activation. Increased EMG activity confirms that muscle recruitment patterns were different between the two co-contraction conditions. Trunk stiffness was determined from impulse response functions (IRFs) analyses of trunk dynamics wherein the kinematics were represented as a second order behavior. Trunk stiffness increased 37.8% ($p < 0.004$) from minimal to maximal co-activation. Results support the assumption used in published models of spine biomechanics that recruitment of trunk muscle co-contraction increases trunk stiffness thereby supporting conclusions from those models that co-contraction contributes to spinal stability.

4.1 Introduction

Muscle stiffness increases with muscle activation as a result of the increased number of activated cross-bridges [25]. Muscle activation has been shown to increase joint stiffness in the elbow [1,32], the ankle [19], and the trunk [27,28]. With co-contraction the activity of the agonist and antagonist muscles increase thereby causing increased joint stiffness [17]. Although biomechanical models of the spine have assumed that recruitment of antagonistic co-contraction causes increased trunk stiffness [8,13] in it has never been empirically demonstrated in the trunk [9].

Trunk stiffness is an important contributor to spinal stability. Stability describes the ability to maintain equilibrium despite the presence of kinematic and/or control disturbances. Although passive tissues contribute to trunk stiffness, the ligamentous spine without active muscular support is unstable [6], therefore trunk stiffness is primarily associated with active muscles of the torso musculature[7]. Research concludes that paraspinal muscle reflexes also contribute to apparent stiffness of a joint by responding to perturbation movements and associated muscle strain with proportional muscle activation [5,14]. The stiffness data reported in the current study is the combined behavior of the active intrinsic muscle stiffness and the reflex response. This is referred to as the “effective stiffness” [4]. Effective stiffness can be accurately measured using small amplitude pseudo-random force disturbances and resulting trunk movement [27].

Empirical measurements demonstrate that trunk stiffness increases with exertion effort and associated muscle activity [4,27]. Clearly recruitment of antagonistic co-contraction must cause an increase in trunk muscle activation of both the antagonist and agonist muscle groups [12]. Therefore, we hypothesize that active trunk stiffness must

increase with co-activation of the torso musculature due to the associated increase in recruitment. The specific aim of the project was to evaluate trunk dynamics, specifically stiffness, using systems identification analyses from data recorded during trunk extension exertions with minimal and maximal voluntary co-contraction recruitment.

4.2 Methods

4.2.1 Experiment

Seventeen subjects with no previous history of LBP participated after signing informed consent approved by the institutional review board at Virginia Tech. The mean (standard deviation) height and mass of the subjects were 175.5 (12.0) cm and 74.3 (14.2) kg respectively.

The experiment consisted of an assessment of trunk stiffness at two recruitment conditions (minimal and maximal voluntary co-contraction) while maintaining constant trunk extension exertions. Subjects were attached to a servomotor (Pacific Scientific, Rockford, IL) via a harness and cable system such that anteriorly directed horizontal loads were applied at the T10 level of the trunk (Figure 4.1). The servomotor applied constant isotonic preloads, which the subject was instructed to resist by maintaining an upright posture. Isotonic loads included 15% and 30% of the subject's maximum voluntary exertion (MVE). MVE force was measured in isometric trunk extension prior to the experiment. Subjects were instructed to maximally recruit their trunk flexor muscles as antagonists during maximum co-contraction trials while maintaining an upright posture against the preload. During minimum co-contraction trials subjects were

instructed to relax their trunk flexor muscles while maintaining an upright posture.

Recruitment and preload conditions were presented in random order.

During the exertions pseudorandom binary (PRB) perturbations of ± 70 N were superimposed on the force preload and were measured with a force transducer (Omega, Stamford, CT) attached to the motor. The force perturbations produced small flexion and extension movements of the trunk that were recorded with electromagnetic position sensors (Ascension Technology Corp., Burlington, VT). Two six degree-of-freedom position sensors were taped to the skin over the spinous process at S1 and T10 and sampled at 100 Hz. Two trials with duration of twenty seconds were performed in each condition. Subjects were instructed to maintain the desired co-contraction effort throughout the trial. Fatigue was minimized by experimental design of low exertion levels, i.e. 15% and 30% MVC and also by requiring at least one minute rest between each trial.

EMG data were collected during each trial to document coactive recruitment. EMG signals were collected from bipolar surface electrodes (Delsys, Boston, MA) on the left and right rectus abdominus (RA), lumbar paraspinal (LP), internal oblique (IO), and external oblique (EO) as described in Granata [11]. All EMG data were band-pass filtered in hardware between 20 and 450 Hz and sampled at 1000 Hz. The EMG signals were rectified and filtered using a 15 Hz, low-pass, seventh-order Butterworth filter. EMG were normalized to their corresponding peak EMG values recorded during maximum isometric flexion, extension, and lateral twisting exertions. Reported EMG recruitment data represents the average isometric baseline value from the first 250 ms of recorded data i.e. during steady state preload and prior to perturbations. All trunk

extension exertions were sagittally symmetric. Preliminary results indicated that there was no significant difference between left and right muscles within each muscle group. Therefore reported muscle recruitment is the average of the left and right muscle of each of the four muscle groups.

4.2.2 Analysis

Prior to system identification, data were processed to ensure accurate calculation of trunk stiffness. Force and displacement signals were filtered using a 75 Hz, low-pass, seventh-order Butterworth filter (Matlab, Natick, MA). Both signals were treated with the same filter to avoid phase shift discrepancy from data processing. The data signals were demeaned prior to analysis to properly estimate the correlation functions [2]. Published techniques illustrate that adding white noise to the input signal reduces the effect of system noise by decorrelating the extraneous noise and data sampling from the input signal [24]. The magnitude of white noise added was 30% of one standard deviation of the input trunk force.

To quantify trunk stiffness, a nonparametric impulse response function (IRF) was estimated using the method of Moorhouse and Granata [27]. The IRF represents the transfer function relating the pseudorandom force input disturbance, $x(t)$, to the T10 displacement output, y_{meas} . IRFs were determined from the matrix solution relating the force autocorrelation function and the force/displacement cross-correlation function [20,27]. This can be written mathematically as:

$$IRF = \frac{1}{\Delta t} C_{xx}^{-1} C_{xy} \quad (4.1)$$

where C_{xx} is the input (force) autocorrelation, C_{xy} is the input/output (force/position) cross-correlation, and Δt is the sample period. To measure the quality of the IRF estimate, it was convolved with the measured pseudorandom force sequence, $x(t)$, to produce an estimate of the trunk displacement, y_{est} . The equivalence between the predicted and observed displacements (Figure 4.2) was measured in terms of the percentage of displacement variance accounted for (VAF), defined as

$$VAF = 100 \left(1 - \frac{\sum (y(t)_{Meas} - y(t)_{Est})^2}{\sum (y(t)_{Est})^2} \right) \quad (4.2)$$

VAF equal to 100% indicates the IRF exactly predicts the measured trunk displacement signal from the input force perturbations.

Inspection of the IRF shapes revealed that dynamics appeared similar to a second-order, underdamped system exhibiting one oscillation (Figure 4.2). Therefore the nonparametric IRFs were subsequently parameterized by determining the coefficients of the second-order system which provided the best least-squares fit to the IRF. The compliance model had the form of:

$$H(s) = \frac{1}{ms^2 + bs + k} \quad (4.3)$$

where m is the effective trunk mass, b is the effective trunk damping, and k is the effective trunk stiffness. The quality of the second-order fit compared with the nonparametric IRF was calculated as a percentage and referred to as model accuracy.

4.2.3 Statistical Analysis

Repeated measures statistical analysis, ANOVA, was performed to determine the effect of co-activation condition and preload on trunk stiffness and recorded muscle recruitment. Significance was determined at the level of $\alpha < 0.05$. Tukey honest-significant difference (HSD) post-hoc analyses were used to compare differences among significant treatments.

4.3 Results

Antagonistic muscle recruitment was successfully achieved as evidenced by significantly increased flexor muscle activity (Figure 4.3). During the maximum co-contraction conditions the RA EMG activity was greater than the minimum co-contraction conditions by 12.5% ($p < 0.005$). Similarly, EO increased by 19.4 % ($p < 0.02$) and IO recruitment increased 7.5% ($p < 0.04$) with co-contraction recruitment. Likewise, LP demonstrated a trend toward increased EMG activity during the maximum co-contraction conditions but failed to reach statistical significance ($p = 0.248$). As expected, baseline extensor muscle activity increased significantly with preload. During the 30% MVC trials the LP activity was 27.5% ($p < 0.03$) greater than during the 15% MVC exertions. Similarly, IO increased 11.9% ($p < 0.01$) with preload. Muscle recruitment in the flexor muscles did statistically change with respect to preload.

IRFs accurately predicted the active trunk kinematic response as evidenced by mean VAF of 79.4 (13.0) %. It is clear by inspection (Figure 4.2) that the second-order model provides an excellent description of the linear trunk dynamics. This was validated

numerically by determining the second-order model accuracy with a mean of 95.2 (3.6) %. Therefore, the analysis accurately represented trunk dynamics.

Trunk stiffness increased 37.8% ($p < 0.004$) with co-contraction recruitment (Table 4.1). Trunk stiffness increased 18.4% ($p < 0.002$) with preload effort. There was a significant ($p < 0.03$) interaction between co-contraction and preload conditions. Within the 15% MVE preload condition the trunk stiffness increased by 56.0% ($p < 0.0002$) with co-contraction recruitment. Co-contraction was associated with a 24.3% increase ($p < 0.001$) in trunk stiffness within the 30% MVE preload condition. Within the minimal co-contraction condition stiffness increased 35.1% with preload ($p < 0.01$). Conversely, preload did not affect stiffness within the maximal co-contraction conditions ($p = 0.33$). This was attributed to the fact that measured activity of the LP muscle group significantly ($p < 0.05$) increased with preload during minimum co-contraction. Measured activity of the LP muscle group was not significantly ($p = 0.128$) different with respect to preload during maximum co-contraction.

Mean effective mass was 47.8 (18.7) kg. Effective mass increased 22.3% with preload effort ($p < 0.03$) but was not statistically affected by co-contraction recruitment. Mean effective damping was 15.4 (4.2) N-m-s/rad and increased 21% with preload ($p < 0.0001$). Effective damping did not change with co-activation condition. Calculating the damping ratio, $\zeta = \frac{b}{2\sqrt{mk}}$ yields a mean value of 0.575 (0.154). Damping ratio did not change with preload effort, but increased 19.2% with co-activation ($p < 0.007$).

4.4 Discussion

Voluntary recruitment of co-contraction in the ankle musculature has been associated with an increase in muscle recruitment of both agonist and antagonist muscle in order to maintain a neutral posture [12,17]. Recognizing that increased muscle activity is associated with greater joint stiffness [22] the co-contraction recruitment about the ankle [17] and elbow[23] was also associated with an increase in joint stiffness. In the trunk, antagonistic co-contraction recruitment in the abdominal musculature generates trunk flexion moment that must be offset by increased activity in extensor muscles to maintain an upright posture. Therefore, results demonstrated increased activity in both trunk flexor and extensor muscle groups during when recruiting voluntary co-contraction of the flexor muscles during trunk extension exertions. Trunk stiffness was quantified as a function of co-contraction effort with results demonstrating that trunk stiffness is greater when antagonistic co-contraction is recruited. Therefore, this study empirically validates the assumption used in published models of spine biomechanics that co-contraction influences trunk stiffness [9].

Increased extension exertion has been shown to increase trunk stiffness presumably due to increased activity and stiffness in the trunk extensor muscles [27]. This effect was confirmed in the current study. Increased preload efforts were associated with increased LP and IO muscle activity as well as significantly increased trunk stiffness. The extent to which the change in trunk stiffness can be attributed to the increased activity in the extensor muscles versus the increased activity in the flexor muscles should be addressed in future research. Significant interaction between recruitment condition and preload level indicates that the potential influence of co-

contraction recruitment is modulated by trunk extension force. At high preload levels there is a limit to the available increase in extensor muscle activity. Recognizing that extensor muscle activity must increase commensurate with antagonistic recruitment to balance the trunk moment, this limits the upper bound of antagonistic co-contraction. Moreover, inhibitory neural pathways have been identified between agonist-antagonist muscle pairs in many joints [29,30] that may limit antagonistic co-contraction recruitment with increase extension effort. Results from the measured EMG support this mechanism. The increase in LP activity associated with preload was less during the maximum co-contraction condition than during the minimum co-contraction condition. Hence the ability to voluntarily modulate trunk stiffness is influenced by preload effort.

Anthropometric data tables suggest that trunk mass is approximately 55% of total body mass [3]. The mean effective mass recorded from the measurement protocol was 64.3% of total mass. Trunk mass should be independent of joint torque [10,19] and therefore independent of co-activation and preload. Results indicated that co-activation did not influence effective mass. However preload level significantly increased effective mass. Effective mass was close to 55% of body mass at the lower preload but was significantly greater at the higher preload. Results suggesting significant changes in effective mass with exertion effort are unexpected. Gardner-Morse and Stokes [31] observed similar effects and concluded that the mass coefficient may not fully describe the inertial effects of the flexible trunk. In a linear second order dynamic model the effective mass parameter represents a mass being rotated about a constant center of rotation (COR). Our analysis makes no assumption about the location of the COR but it assumes the location is constant. We are unaware of any study to determine whether the

instantaneous COR of the lumbar spine changes with extension effort. Results suggest the COR in the sagittal plane of the trunk may be a function of extension effort. If COR moves caudally with increased trunk extension effort, then trunk dynamics will demonstrate greater effective driving point mass due to the decreased moment arm from the COR to the center of mass. Further research is necessary to understand this phenomenon. Fortunately the analyses were capable of solving separately for effective mass and stiffness, therefore our concerns regarding mass should not influence stiffness results.

An increase in effective damping was to be expected [15,16,27]. Joint stiffness and joint damping tend to increase in such a way as to maintain a constant damping ratio [22]. Our results were consistent with the literature in this regard, i.e. damping ratio was independent of preload effort. The joint dynamics described above, such as the constant damping ratio, are technically valid only for exertions without co-contraction [22]. However, results show that damping ratio increased with co-contraction. Hunter and Kearney [22] acknowledge that coactive recruitment can change joint dynamics and observed this effect in the ankle [18]. The ability to voluntarily modulate trunk dynamics by means of stiffness and damping ratio provides robust neuromuscular control throughout a variety of dynamic loading conditions.

Results must be considered in light of methodological limitations. The constant perturbation force used in the current study may cause different magnitudes of motion response between different subjects and preload conditions. The small angle kinematic response to the force perturbations is influenced by the mass and stiffness of the system. Hence, anthropometry and preload effort may influence the muscular reflex response and

its associated contribution to effective stiffness. It is suggested that instead of using force perturbations, future research should investigate stochastic position perturbations. Trunk stiffness results include the effects from both intrinsic muscle stiffness and reflex contributions to trunk dynamics. Improved analysis techniques should be applied to separate trunk stiffness into its intrinsic and reflexive components [21].

This study confirms that torso dynamics are influenced by recruitment co-contraction. Accurate estimates of joint dynamics parameters must therefore include effects of coactive recruitment. Biomechanical models of spinal stability suggest that antagonistic co-contraction can be used to augment stability by increasing the net bending stiffening of the spinal column[8,13,26]. Our empirical measurements support those conclusions by demonstrating that antagonistic co-contraction can be used to augment trunk stiffness. Existing stability models of the spine are typically limited to static stability analyses. Current results suggest damping ratio of trunk dynamics can be modulated voluntarily. Thus, future analyses should investigate the voluntary control of dynamic biomechanical stability of the lumbar spine.

4.5 Acknowledgement

This research was supported in part by a grant R01 AR49932 from CDC / National Institute for Occupational Safety and Health.

4.6 References

1. Agarwal G.C. and Gottlieb G.L. Compliance of the human ankle joint. *J Biomech.Eng.* 99 (1977) 166-170.
2. Bendat,J.S. and Piersol,A.G. (2000) *Random data: analysis and measurement procedures.*, John Wiley & Sons, New York
3. Chaffin,D.B., Stump,B.S., Nussbaum,M.A. and Baker,G. Low-back stresses when learning to use a materials handling device. *Ergonomics* 42 (1999) 94-110.
4. Cholewicki,J., Simons,A.P.D. and Radebold,A. Effects of external trunk loads on lumbar spine stability. *J.Biomechanics* 33 (2000) 1377-1385.
5. Crago P.E., Houk J.C. and Hasan Z. Regulatory actions of human stretch reflex. *J.Neurophysiol.* 39 (1976) 925-935.
6. Crisco,J.J. and Panjabi,M.M. Euler stability of the human ligamentous lumbar spine: Part I Theory. *Clin.Biomech.* 7 (1992) 19-26.
7. Dolan P., Earley M. and Adams M.A. Bending and compressive stresses acting on the lumbar spine during lifting activities. *J.Biomechanics* 27 (1994) 1237-1248.
8. Gardner-Morse,M.G. and Stokes,I.A.F. The effects of abdominal muscle coactivation on lumbar spine stability. *Spine* 23 (1998) 86-92.
9. Gardner-Morse,M.G., Stokes,I.A.F. and Laible,J.P. Role of muscles in lumbar stability in maximum extension efforts. *J.Orthop.Res.* 13 (1995) 802-808.
10. Gottlieb G.L., Song Q., Almeida G.L., Hong D.A and Corcos D. Directional control of planar human arm movement. *J.Neurophysiol.* 78 (1997) 2985-2998.
11. Granata,K.P. and Marras,W.S. An EMG assisted model of biomechanical trunk loading during free-dynamic lifting. *J.Biomechanics* 28 (1995) 1309-1317.
12. Granata,K.P. and Marras,W.S. The influence of trunk muscle coactivity upon dynamic spinal loads. *Spine* 20 (1995) 913-919.
13. Granata,K.P. and Orishimo,K. Response of Trunk Muscle Coactivation to Changes in Spinal Stability. *J.Biomechanics* 34 (2001) 1117-1123.
14. Granata,K.P., Slota,G.P., Bennett,B.E. and Kang,H.G. Paraspinal muscle reflex dynamics. *J.Biomechanics* 37 (2004) 241-247.
15. Granata,K.P., Slota,G.P. and Wilson,S.E. Influence of fatigue in neuromuscular control of spinal stability. *Hum.Factors* 46 (2004) 81-91.

16. Granata,K.P. and Wilson,S.E. Trunk Posture and Spinal Stability. *J.Biomechanics* 16 (2001) 650-659.
17. Granata,K.P., Wilson,S.E., Massimini,A.K. and Gabriel,R. Active stiffness of the ankle in response to inertial and elastic loads. *J Electromyogr.Kinesiol.* 14 (2004) 599-609.
18. Hunter I., Kearney R.E. and Weiss P.L. Stiffness-torque-EMG relations at various tibialis anterior and triceps surae co-contraction levels obtained by real-time feedback of elastic stiffness. *Soc.Neurosci.Abstr.* 10 (1984) 334.
19. Hunter I.W. and Kearney R.E. Dynamics of human ankle stiffness: Variation with mean ankle torque. *J.Biomechanics* 15 (1982) 747-752.
20. Hunter,I.W. and Kearney,R.E. Two-sided linear filter identification. *Med.Biol.Eng Comput.* 21 (1983) 203-209.
21. Kearney R.E. and Stein R.B. Identification of intrinsic and reflex contributions to human ankle stiffness dynamics. *IEEE Trans.Biomed.Eng* 44 (1997) 493-504.
22. Kearney,R.E. and Hunter,I.W. System Identification of Human Joint Dynamics. *Crit.Rev.Biomed.Eng.* 18 (1990) 55-87.
23. Lacquaniti F., Licata F. and Soechting J.F. The mechanical behavior of the human forearm in response to the transient perturbations. *Biol.Cybern.* 44 (1982) 35-46.
24. Ljung,L. and Ljung,E.J. (1998) *System Identification: Theory for the User*, Prentice Hall, Upper Saddle River, NJ
25. Ma,S.P. and Zahalak,G.I. The mechanical response of the active human triceps brachii muscle to very rapid stretch and shortening. *J.Biomech.* 18 (1985) 585-598.
26. Meakin J.R., Hukins D.W. and Aspden R.M. Euler buckling as a model for the curvature and flexion of the human lumbar spine. *Proc.Roy.Soc.Lond.B* 263 (1996) 1383-1387.
27. Moorhouse, K. M. and Granata, K. P. Trunk stiffness and dynamics during active extension exertions. *J.Biomechanics* . 2004.
Ref Type: In Press
28. Moorhouse, K. M., Kaufman, G., and Granata, K. P. Parametric Deconvolution for Calculation of Dynamic Trunk Stiffness. 2004. *Intl.Soc.Electromyo.Kinesiol.*
Ref Type: Conference Proceeding
29. Myklebust B.M., Gottlieb G.L., Penn R.D. and Agarwal G.C. Reciprocal excitation of antagonist muscles as a differentiating feature in spasticity. *Ann.Neurol.* 12 (1982) 367-374.

30. Simon,S.R. (1994) Orthopaedic Basic Science, Am.Acad.Orthop.Surg., Rosemont, IL
31. Stokes,I.A.F., Gardner-Morse,M.G., Henry,S.M. and Badger,G.J. Decrease in trunk muscular response to perturbation with preactivation of lumbar spinal musculature. Spine 25 (2000) 1957-1964.
32. Zhang,L.Q. and Rymer,W.Z. Simultaneous and nonlinear identification of mechanical and reflex properties of human elbow joint muscles. IEEE Trans.Biomed.Eng 44 (1997) 1192-1209.

4.7 Figures and Tables

Figure 4.1. Experimental setup. Force perturbations in a pseudo-random fashion superimposed on isotonic loads were applied to subjects to elicit small trunk movement during two co-activation conditions (maximal and minimal voluntary recruitment of flexor muscles). Subjects were securely strapped into a rigid pelvic support structure to isolate movement of the trunk for all trials.

Figure 4.2. IRFs relating trunk displacement to the applied trunk force during maximal and minimal co-activation and the superimposed second-order least-mean-squares fit. This clearly illustrates that a linear second-order model can accurately describe the trunk dynamics. Conditions represent maximum co-activation (a) and minimum co-activation (b) and demonstrate differences in trunk stiffness.

Figure 4.3. Comparison of EMG activity with co-activation. Muscle activity in the rectus abdominus (RA), external oblique (EO), and internal oblique (IO) increased significantly ($p < 0.05$) during maximum co-activation as denoted with *.

Table 4.1. Trunk stiffness during active voluntary exertions.

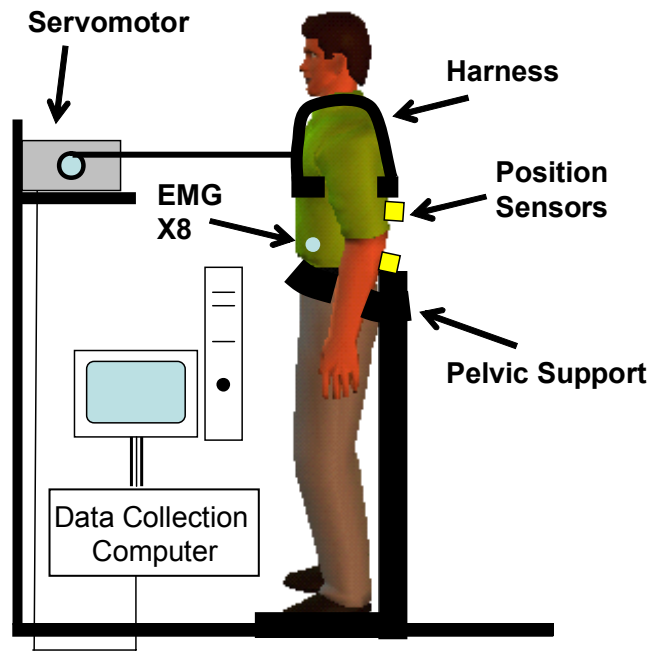


Figure 4.1. Experimental setup. Force perturbations in a pseudo-random fashion superimposed on isotonic loads were applied to subjects to elicit small trunk movement during two co-activation conditions (maximal and minimal voluntary recruitment of flexor muscles). Subjects were securely strapped into a rigid pelvic support structure to isolate movement of the trunk for all trials.

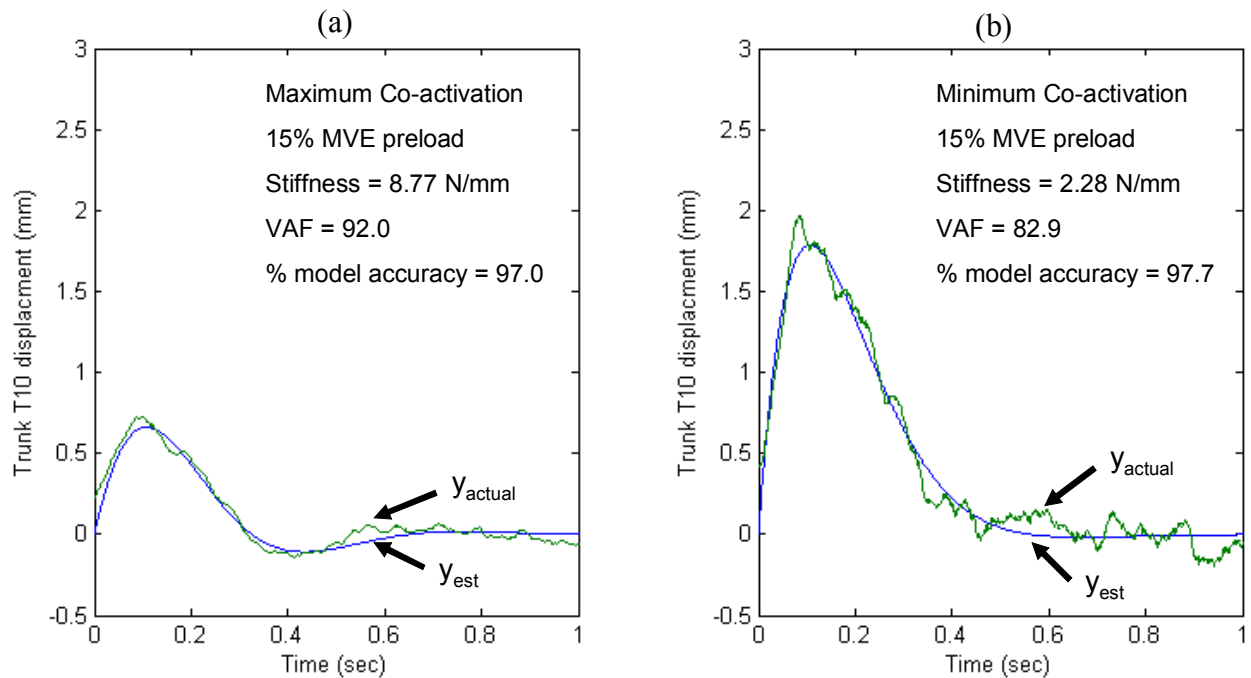


Figure 4.2. IRFs relating trunk displacement to the applied trunk force during maximal and minimal co-activation and the superimposed second-order least-mean-squares fit. This clearly illustrates that a linear second-order model can accurately describe the trunk dynamics. Conditions represent maximum co-activation (a) and minimum co-activation (b) and demonstrate differences in trunk stiffness.

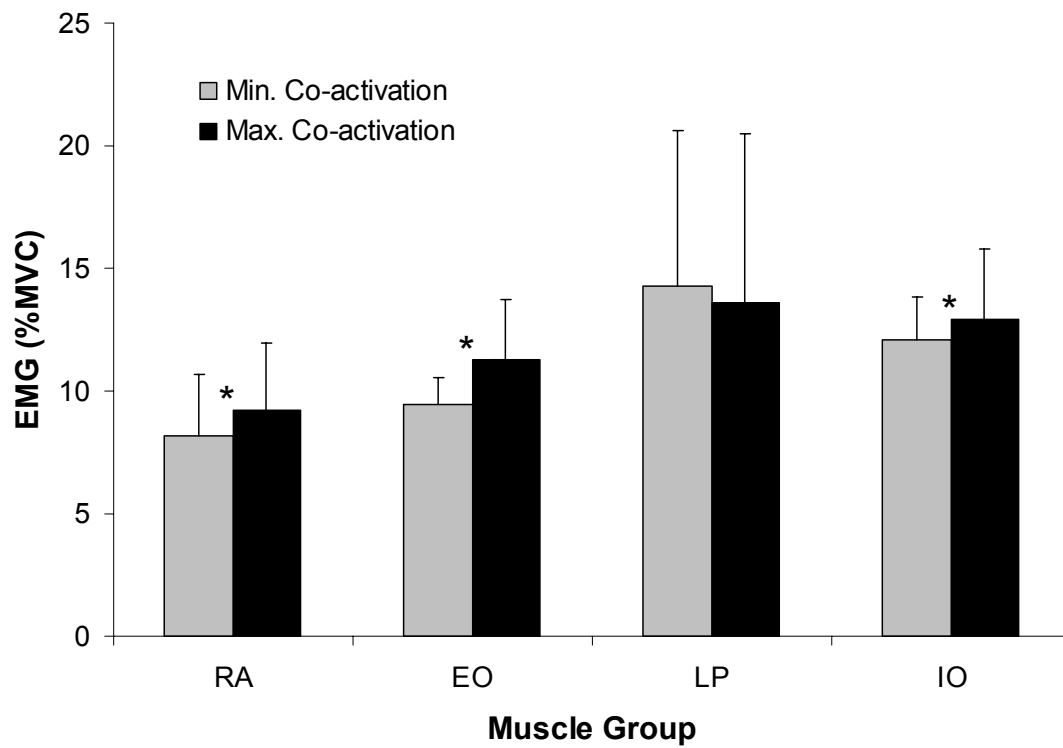


Figure 4.3. Comparison of EMG activity with co-activation. Muscle activity in the rectus abdominus (RA), external oblique (EO), and internal oblique (IO) increased significantly ($p < 0.05$) during maximum co-activation as denoted with *.

Table 4.1. Trunk Stiffness during active voluntary exertions				
	15 % of MVE	30 % of MVE	Average	
<i>Stiffness (N/mm)</i>				
Maximum Co-activation	4.87 (1.81) ^b	5.24 (1.98) ^b	5.05 (1.87) ^a	
Minimum Co-activation	3.12 (1.12) ^{b d}	4.22 (1.66) ^{b d}	3.67 (1.50) ^a	
Average	3.99 (1.72) ^c	4.73 (1.88) ^c	4.36 (1.83)	
Mean (standard deviation) of stiffness. Results show main effects for two-way interactions on stiffness.				
^a Significant main effect for co-activation p < 0.05.				
^b Significant effect of co-activation within preload level p < 0.05.				
^c Significant main effect for preload p < 0.05.				
^d Significant effect of preload within co-activation condition p < 0.05.				

CHAPTER 5

ACTIVE TRUNK STIFFNESS DURING VOLUNTARY ISOMETRIC FLEXION AND EXTENSION EXERTIONS

Submitted to: *European Spine Journal*

21 December 2004

Patrick J. Lee

Kevin P. Granata, Ph.D.

Musculoskeletal Biomechanics Laboratories
Department of Engineering Science & Mechanics
School of Biomedical Engineering & Science
Virginia Polytechnic Institute & State University
219 Norris Hall (0219)
Blacksburg, VA 24061

Address all correspondence to: K.P. Granata, Ph.D.
Musculoskeletal Biomechanics Laboratories
Department of Engineering Science & Mechanics
Virginia Polytechnic Institute & State University
219 Norris Hall (0219)
Blacksburg, VA 24061
Phone: (540) 231-5316
FAX: (540) 231-4547
Granata@VT.edu

KEYWORDS : Low-Back, Spine, Stiffness, Co-contraction, Push

Abstract

Co-contraction has been shown to be twice as higher during isometric trunk flexion compared to extension. Co-contraction is also associated with higher biomechanical stiffness. Conversely, past studies have not found a statistical difference between trunk stiffness in flexion and extension exertions. The goal of this study was to investigate this paradox. Twelve subjects maintained an upright trunk posture against an external flexion or extension load applied to the trunk. Pseudo-random stochastic force sequences were superimposed on the isotonic preloads causing small amplitude trunk movements. Nonparametric impulse response functions (IRFs) of trunk dynamics were computed and revealed that the system exhibited underdamped second-order behavior. Second order dynamics were determined by calculating the best least-squares fit to the IRF. Trunk stiffness was significantly greater ($p < 0.05$) during flexion exertions compared to extension exertions. EMG data were recorded from left and right rectus abdominus (RA), external obliques (EO), lumbar paraspinal (LP), and internal oblique (IO) to quantify co-contraction associated with trunk stiffness. EMG was greater in both agonist and antagonist muscle during flexion exertions. Results suggest the co-contraction associated with trunk flexion exertions is associated with increased trunk stiffness compared to extension exertions. Trunk stiffness and recruitment were attributed to neuromuscular control of spinal stability. Future studies need to consider neuromuscular control of spinal stability when evaluating the biomechanical risks of trunk flexion and extension exertions.

5.1 Introduction

During pushing tasks or flexion exertions the lumbar paraspinal (LP) and posterior internal oblique (IO) muscles provide little mechanical potential for the generation of torso flexion moment [2,23]. They are therefore considered antagonistic with respect to the flexion exertion. However, co-contraction of the lumbar paraspinal muscles during pushing exertions may be necessary to augment spinal stability [7,12]. The ligamentous spine without active muscular support is unstable at compressive loads greater than 88 N [8] yet compressive forces on the spine can exceed 3400 N during lifting tasks [15] and 1400 N during pushing tasks [29]. Although passive tissues contribute to trunk stiffness, in upright postures the passive tissue contribution is small so trunk dynamics are primarily associated with stiffness of active muscles [10,27,28]. Active stiffness of the torso musculature acts to return the spine to an equilibrium state following a kinematic disturbance thereby contributing to spinal stability. Therefore, theoretical analyses suggest that co-contraction in the LP muscles must be recruited during trunk flexion exertions to maintain lumbar spine stability [16]. Empirical measurements support this assertion, demonstrating that co-contraction during flexion exertions is twice the co-contraction during trunk extension exertions [4,14]. Recognizing that co-contraction contributes to stiffness [6,11,17], the trunk stiffness should be greater during flexion exertions than during extension exertions. This is contrary to past investigations which have found no difference in trunk stiffness between flexion and extension exertions [6,11]. Therefore, the goal of this study was to investigate this paradox by experimental measurement of trunk stiffness during voluntary trunk flexion and extension exertions using high-bandwidth, stochastic measurement of torso dynamics.

Measurements of trunk stiffness during active voluntary flexion and extension exertions have been reported using various perturbation methods. Cholewicki [6] used a linear second-order model to estimate stiffness from trunk movement subsequent to a sudden change in equilibrium force. They reported no significant difference in trunk stiffness during flexion exertions compared to extension exertions. However, linear second-order estimates of trunk dynamics are applicable only for small disturbances about a constant equilibrium moment. Since there was a large change in trunk moment, equilibrium was different before and after the disturbance making it difficult to differentiate between effects of equilibrium and stiffness. To avoid a change in equilibrium moment Gardner-Morse and Stokes [11] applied single-period, sinusoidal force perturbations while subjects maintain steady-state voluntary trunk flexion and extension efforts. No differences in stiffness between flexion and extension exertions were reported. Moorhouse and Granata [26] used systems identification analyses to estimate trunk stiffness from small amplitude pseudo-random force disturbances and resulting trunk movement. The advantages of this approach are that pseudo-random stochastic inputs avoid problems with voluntary responses due to predictable stimuli [21], it allows steady-state equilibrium during the measurement protocol, and the perturbations apply a flat disturbance bandwidth from 0-10 Hz [26]. Although internal validity measures indicate accurate representation of trunk dynamics, only trunk extension exertions were examined. Comparison of trunk stiffness during voluntary flexion and extension exertions require further measurements.

We hypothesize that trunk stiffness during steady-state trunk flexion exertions must be greater than trunk stiffness during equivalent trunk extension exertions. We attribute

this difference to the increased levels of co-contraction during flexion exertions with respect to co-contraction levels observed during extension tasks [14]. The specific aim of the project was to evaluate trunk dynamics, including mass, damping and stiffness using systems identification analyses from data recorded during flexion and extension exertions.

5.2 Methods

5.2.1 Experiment

Twelve subjects with no history of low back disorders (LBDs) voluntarily participated in this experiment. Mean (\pm standard deviation) subject mass and stature was 71.4 ± 21.3 kg and 175.1 ± 9.8 cm. respectively. Before participation, all subjects signed informed consent approved by the Virginia Tech human subjects review board.

The protocol required subjects to maintain an upright trunk posture against an external flexion or extension load applied to the trunk. Subjects were secured to a pelvic restraint frame designed to restrict the motion of the pelvis and lower body while in a standing posture (Figure 5.1). A chest harness and cable system attached the subject to a servomotor (Pacific Scientific, Rockford, IL) such that cable tension applied external loads at the T10 level of the trunk. The motor applied isotonic loads of 100, 135, and 170 N. To generate trunk extension exertions the subjects faced the motor such that the cable tension applied a horizontal flexion force. To generate trunk flexion exertions the subjects faced away from the motor such that the cable tension applied a horizontal extension force. Superimposed on the external load were force perturbations of ± 30 N

applied in a pseudo-random stochastic fashion with a flat bandwidth from 0-10 Hz.

Three pseudorandom perturbation trials of ten seconds each were performed during both flexion and extension exertions and at each exertion force level for a total of eighteen trials per subject presented in random order.

The applied forces were measured by a force transducer (Omega, Stamford, CT) attached to the shaft of the motor and sampled at 1000 Hz. The small amplitude dynamic trunk movement was recorded using two OPTOTRAK infrared emitting diodes (Northern Digital, Waterloo, Ontario, Canada). Sensors were taped to the skin surface over the spinous process at the S1 and T10 level of the trunk and were recorded at 200 Hz using a 16 channel A/D converter (Northern Digital, Ontario, Canada). EMG data were collected from bipolar surface electrodes (Delsys, Boston, MA) on the left and right rectus abdomini (RA), LP, internal oblique (IO), and external oblique (EO) as described in Granata [15]. Briefly, electrodes for the RA were placed 3 cm lateral and 2 cm superior to the umbilicus; LP 4 cm lateral to the L3 spinous process; posterior IO 8 cm lateral to the midline within the lumbar triangle at a 45⁰; and EO 10 cm lateral to the umbilicus with an orientation of 45⁰ to vertical. All EMG data were band-pass filtered in hardware between 20 and 500 Hz and sampled at 1000 Hz. The EMG signals were rectified and filtered using a 25 Hz, low-pass, seventh-order Butterworth filter (Matlab, Natick, MA). EMG signals from each muscle were normalized to their corresponding peak EMG value recorded during maximum isometric flexion, extension, left and right-lateral twisting. Mean baseline EMG was recorded during the isometric exertions in a 250 msec period prior to initiation of the force perturbations. Reported muscle activity is the average of the left and right muscle of each of the four muscle groups because preliminary results

indicated that there was no significant difference between left and right muscle activity within each condition.

5.2.2 Analysis

To quantify trunk stiffness, the nonparametric compliance impulse response function (IRF) was estimated. The IRF represents the transfer function relating the pseudorandom force disturbance input, $x(t)$, to the T10 displacement output, y_{meas} . Both the applied trunk force data and trunk displacement data were filtered using a 75 Hz, low-pass, seventh-order Butterworth filter (Matlab, Natick, MA) and sub-sampled to 200 Hz. Both the force and displacement signals were treated with the same filter to avoid phase shift discrepancy from data processing. Both the applied trunk force and the trunk displacement were demeaned prior to analysis in order to properly estimate the correlation functions [3]. Published techniques illustrate that adding white noise to the input signal reduces the effect of system noise by decorrelating the extraneous noise and data sampling from the input signal [25]. The magnitude of white noise added was 30% of one standard deviation of the input trunk force.

IRFs were determined from the matrix solution relating the autocorrelation function of the force signal and the cross-correlation of the force/displacement signals [18,26]. This can be written mathematically as:

$$IRF = \frac{1}{\Delta t} C_{xx}^{-1} C_{xy} \quad (5.1)$$

where C_{xx} is the input (force) autocorrelation, C_{xy} is the input/output (force/position) cross-correlation, and Δt is the sample period. To measure the quality of the IRF estimate, it was convolved with the measured pseudorandom force sequence, $x(t)$, to produce an estimate of the trunk displacement, y_{est} . The equivalence between the predicted and observed displacements was measured in terms of the percentage of displacement variance accounted for (VAF), defined as

$$VAF = 100 \left(1 - \frac{\sum (y(t)_{Meas} - y(t)_{Est})^2}{\sum (y(t)_{Est})^2} \right) \quad (5.2)$$

VAF equal to 100% indicates the IRF exactly predicts the measured trunk displacement signal from the input force perturbations.

The force and displacement data were visually inspected for signal quality. Five of the 216 trials collected were removed due to sections of missing kinematic data presumably caused by the subject's clothing, hair, or harness blocking the infrared emitting diode. Thirteen trials had VAF less than 70% and were removed prior to statistical analysis. Concatenation of the trials at each exertion level and direction provides more robust system identification [21]. Thus, 198 of the original 216 trials were retained to form 72 compliance IRFs (six per subject) used for parametric analysis.

Inspection of the IRF shapes revealed dynamics that appeared similar to a second-order, underdamped system exhibiting one oscillation (Figure 5.2). Therefore the nonparametric IRFs were subsequently parameterized by determining the coefficients of the second-order system which provided the best least-squares fit to the IRF. The compliance model had the form of:

$$IRF = \frac{1}{ms^2 + bs + k} \quad (5.3)$$

where m is the effective trunk mass, b is the effective trunk damping, and k is the effective trunk stiffness. The parameters were described as effective stiffness, damping, and mass because the data represented combined behaviors from intrinsic stiffness and reflex stiffness, with similar effects of damping, while the effective mass represented the driving point mass recorded by the systems identification technique measured at the T10 level of the trunk. The quality of the second-order fit compared with the nonparametric IRF was calculated as a percentage and referred to as fit accuracy.

5.2.3 Statistical Analysis

Statistical analyses were performed to determine the effects of flexion/extension direction and exertion level (100 N, 135 N, 170 N) on trunk stiffness and trunk muscle activity. A two factor (flexion/extension and exertion level) repeated measures ANOVA were performed on trunk stiffness and activity of each of the four bilateral muscle groups. Analyses were performed using commercial software (Statistica, 4.5 Statsoft, Inc., Tulsa OK) using a significance level of $\alpha < 0.05$.

5.3 Results

RA and EO were the primary muscles responsible for generating the flexion moment but results demonstrates notable antagonistic co-activation in IO and LP during the flexion exertions. RA activity was 36.4% greater during flexion than during

extension ($p < 0.05$). IO activity increased 16.6% ($p < 0.05$) and EO increased 76.0% ($p < 0.01$) during flexion versus extension exertions (Figure 5.3). Muscle activity of the LP was not statistically different ($p = 0.231$) between flexion and extension trials. EMG increased significantly with respect to exertion level in all muscle groups. From the lowest to highest load the recruitment of RA increased 9.9% ($p < 0.05$), IO increased 27.6% ($p < 0.05$), LP increased 17.9% ($p < 0.01$), and EO increased 30.2% ($p < 0.01$).

Compliance IRFs accurately predicted the active trunk kinematic response to random perturbation forces as evidenced by mean VAF of $88.9 \pm 5.1\%$. It is clear by inspection (Figure 5.2) that the second-order model provides an excellent description of the trunk dynamics. This was validated numerically by determining the second-order fit accuracy with a mean value of $89.4 \pm 7.0\%$.

Trunk stiffness was significantly ($p < 0.05$) greater during flexion exertions than during extension exertions with mean values of 5.00 ± 1.65 N/mm and 4.11 ± 1.28 N/mm respectively (Figure 4). Trunk stiffness increased 54.2% from the lowest to highest exertion level ($p < 0.01$). Mean stiffness was 3.53 ± 0.97 N/mm during 100 N exertions and 5.99 ± 1.59 N/mm during 170 N conditions. There was no significant interaction between load direction and exertion level on trunk stiffness ($p = 0.487$).

Effective trunk damping was significantly greater during flexion exertions than during extension exertions with means of 445 ± 121 and 827 ± 360 N-s/m respectively ($p < 0.01$). Damping increased 42.3% from the lowest to highest exertion with means of 517 ± 273 to 736 ± 380 N-s/m respectively ($p < 0.01$). Mean effective mass was 46.3 ± 24.6 kg and represented the apparent driving point load. The mean effective mass was significantly greater ($p < 0.01$) during flexion exertions, 53.2 ± 19.4 kg, compared to

extension exertions, 39.5 ± 10.8 kg. This effective mass was significantly ($p < 0.01$) greater during 170 N exertions than during 100 N exertions. The mean mass at the lowest load level was 33.9 ± 22.0 kg compared to 58.8 ± 34.4 kg at the highest exertion level.

5.4 Discussion

The effect of load direction on active trunk stiffness was evaluated using a pseudo-random disturbance and system identification methods. Nonparametric IRFs of trunk dynamics were computed and revealed that the system exhibited underdamped second-order behavior. The behavior agrees with previously published studies of trunk dynamics [6,11,26] and readily allows interpretation of perturbation response in terms of effective mass, damping and stiffness of the trunk. Trends in trunk stiffness with voluntary exertion effort agreed with published data. Studies report that active muscle [19] and joint stiffness [21] increase with muscle activation. Likewise, it has been noted elsewhere that stiffness of the trunk increases with exertions level [6,11,26]. Results from the current study similarly observed a significant increase in trunk stiffness with exertion. Results also reveal greater trunk stiffness during flexion exertions than during extension exertions.

Greater trunk stiffness during flexion exertions than during extension exertions was attributed to muscle co-activation. During flexion exertions the RA and EO muscles provide mechanical potential for the generation of torso flexion. Results demonstrated significantly increased activity in these muscles during flexion exertions compared to similar extension exertion efforts (Figure 5.4). We also observed significantly greater IO

activity during flexion exertions than during extension exertions. Moreover, during flexion exertions the activity in the LP muscles was not statically different than activity recorded during extension exertions. This indicates notable antagonistic co-contraction during flexion exertions in these extensor muscles. In recent studies we have reported that co-contraction of the lumbar paraspinal muscles during pushing exertions may be necessary to augment spinal stability [14,16]. Results from those and other [4] studies conclude that co-contraction during flexion exertions is twice the co-contraction during trunk extension exertions. Recognizing that muscle stiffness increases with activation [19], and that co-contraction is associated with increased muscle activation in both the agonist and antagonist muscles, then active joint rotational must increase with co-contraction. This has been demonstrated in the ankle [17,21], elbow [22] and in the torso [5,24]. Hence, during flexion and extension exertions of similar effort, we observed increased trunk stiffness in the condition with the greater co-contraction, i.e. greater trunk stiffness in flexion exertions than during extension exertions. However, this does not agree with published results wherein others have reported no significant difference in flexion trunk stiffness versus extension trunk stiffness [6,11].

Reasons why differences in trunk flexion and extension stiffness were observed in the current results but not in previous studies may be related to differences in experimental protocols. Analysis of trunk stiffness by means of non-parametric systems identification techniques and parametric modeling provides accurate and robust estimation of trunk dynamics. Nonparametric VAF and parametric fit accuracy values were typically greater than 88% thereby indicating that the estimated values of effective mass, damping and stiffness sufficiently represented the relation between force

disturbance and subsequent trunk movement. Consequently, analyses [26] have demonstrated notably less variability in the stiffness estimates using this techniques than reported elsewhere [6,11]. Mean extension stiffness was approximately 18% less than the trunk stiffness during flexion exertions. Using the sudden load technique [6] to quantify stiffness the standard deviation of trunk stiffness was nearly 50% of the mean values thereby limiting the ability to observe statistical effects of flexion versus extension stiffness. However, recent analyses by Anderson [1] using a similar sudden load technique reported stiffness measurements with much lower variability. Stiffness of the trunk reported by Gardner-Morse and Stokes [11] was evaluated using sinusoidal disturbances at 4 Hz. Subsequently analyses demonstrate that trunk dynamics possess a resonant frequency of approximately 1 Hz [26]. Hence, the 4 Hz protocol estimated trunk dynamics at a point on the bandwidth that is most sensitive to mass and reflex but may be comparatively less sensitive to subtle changes in stiffness. Thus, when evaluating change in neuromuscular control of stability and active stiffness, we recommend protocols using large disturbance bandwidth, e.g. 0 to 10 Hz, and small disturbances about a constant baseline equilibrium force and angle.

Study limitations should be considered when interpreting the results. The measured stiffness included components of passive tissue stiffness, intrinsic active muscle stiffness and reflex dynamics. Reflex dynamics may contribute up to 40% of the measured stiffness [17,20,30]. However, we are unaware of any studies that attempt to quantify reflex contributions to trunk stiffness. Therefore, it is unknown whether observed differences in trunk stiffness during flexion and extension exertions are associated with intrinsic or reflex behaviors. Results demonstrate that stiffness increased

with exertion thereby indicating nonlinear behavior of the system. Hence, use of a linear second-order analysis is limited to the neighborhood of the equilibrium recorded in experiment. Extrapolation of these results to notably different exertion levels or postures may not be warranted. Results suggesting significant changes in effective mass with exertion effort and direction are alarming. Gardner-Morse and Stokes [11] observed similar effects and concluded that the mass coefficient may not fully describe the inertial effects of the flexible trunk. Hence, in the current study, the effective center of rotation of the trunk in response to the force disturbances may have been different in flexion and extension exertions. Further research is necessary to understand this phenomenon. Fortunately, the analyses were capable of solving separately for effective mass and stiffness, so the effects of mass should not influence stiffness results. However, the applied force disturbances may cause greater movement in subjects with smaller mass. Stiffness is nonlinearly related to disturbance amplitude [21] indicating small effects highlighting the nonlinear behavior of trunk dynamics. Further studies are recommended to apply nonlinear systems identification methods in order to quantify trunk dynamics during voluntary exertions.

5.5 Conclusions

The results of this study support the importance of co-contraction to maintain spinal stability during flexion exertions. Analyses of pushing tasks report less spinal compression than during lifting exertions [9,29] but often overlook the effects of co-contraction and stability. Theoretical analyses indicate that antagonistic co-contraction in the LP and IO muscles during trunk flexion exertions may be necessary to stiffen the

spine so as to maintain spinal stability [13]. Recent analyses confirm that significant co-contraction is recruited during trunk flexion exertions [14] and the current study supports the hypothesis that the trunk is stiffened during flexion exertions. Results underscore the need to consider co-contraction and neuromuscular control of spinal stability when evaluating the biomechanical risks of trunk flexion and extension exertions.

5.6 Acknowledgement

This research was supported in part by a grant R01 AR49932 from CDC / National Institute for Occupational Safety and Health.

5.7 References

1. Andersen, T.B., Essendrop, M. and Schibye, B. (2004) Movement of the upper body and muscle activity patterns following a rapidly applied load: the influence of pre-load alterations. *Eur.J Appl.Physiol* 91: 488-492.
2. Andres R.O. and Chaffin D.B. (1991) Validation of a biodynamic model of pushing and pulling. *J.Biomechanics* 24: 1033-1045.
3. Bendat, J.S. and Piersol, A.G. (2000) Random data: analysis and measurement procedures., John Wiley & Sons, New York
4. Choi, H. (2003) Quantitative assessment of co-contraction in cervical musculature. *Med.Eng Phys.* 25: 133-140.
5. Cholewicki, J., Juluru, K., Radebold, A., Panjabi, M.M. and McGill, S.M. (1999) Lumbar spine stability can be augmented with an abdominal belt and/or increased intra-abdominal pressure. *Eur.Spine J.* 8: 388-395.
6. Cholewicki, J., Simons, A.P.D. and Radebold, A. (2000) Effects of external trunk loads on lumbar spine stability. *J.Biomechanics* 33: 1377-1385.
7. Crisco, J.J. and Panjabi, M.M. (1991) The intersegmental and multisegmental muscles of the lumbar spine: A biomechanical model comparing lateral stabilizing potential. *Spine* 16: 793-799.

8. Crisco,J.J., Panjabi,M.M., Yamamoto,I. and Oxland,T.R. (1992) Euler stability of the human ligamentous lumbar spine. Part II Experiment. Clin.Biomech. 7: 27-32.
9. deLooze M.P., van Greuningen K., Rebel J., Kingma I. and Kuijer P.P. (2000) Force direction and physical load in dynamic pushing and pulling. Ergonomics 43: 377-390.
10. Dolan,P., Mannion,A.F. and Adams,M.A. (1994) Passive tissues help the back muscles to generate extensor moments during lifting. J.Biomechanics; 27: 1077-1085.
11. Gardner-Morse,M.G. and Stokes,I.A.F. (2001) Trunk stiffness increases with steady-state effort. Journal of Biomechanics 34: 457-463.
12. Gardner-Morse,M.G., Stokes,I.A.F. and Laible,J.P. (1995) Role of muscles in lumbar stability in maximum extension efforts. J.Orthop.Res. 13: 802-808.
13. Granata, K. P. and Bennett, B. E. Low-back biomechanics and stability during pushing. Hum.Factors . 2004. Ref Type: In Press
14. Granata, K. P., Lee, P. E., and Rogers, E. Co-Contraction Recruitment and Spinal Load during Isometric Trunk Flexion. J.Biomech. 2004. Ref Type: In Press
15. Granata,K.P. and Marras,W.S. (1995) An EMG assisted model of biomechanical trunk loading during free-dynamic lifting. J.Biomechanics 28: 1309-1317.
16. Granata,K.P., Slota,G.P., Bennett,B.E. and Kang,H.G. (2004) Paraspinal muscle reflex dynamics. J.Biomechanics 37: 241-247.
17. Granata,K.P., Wilson,S.E., Massimini,A.K. and Gabriel,R. (2004) Active stiffness of the ankle in response to inertial and elastic loads. J Electromyogr.Kinesiol. 14: 599-609.
18. Hunter,I.W. and Kearney,R.E. (1983) Two-sided linear filter identification. Med.Biol.Eng Comput. 21: 203-209.
19. Julian F.J. and Morgan D.L. (1981) Variations of muscle stiffness with tension during tension transients and constant velocity shortening in the frog. J.Physiol. 319: 193-203.
20. Kearney R.E. and Stein R.B. (1997) Identification of intrinsic and reflex contributions to human ankle stiffness dynamics. IEEE Trans.Biomed.Eng 44: 493-504.
21. Kearney,R.E. and Hunter,I.W. (1990) System Identification of Human Joint Dynamics. Crit.Rev.Biomed.Eng. 18: 55-87.

22. Lacquaniti F., Licata F. and Soechting J.F. (1982) The mechanical behavior of the human forearm in response to the transient perturbations. *Biol.Cybern.* 44: 35-46.
23. Lee K.S., Chaffin D.B., Waikar A.M. and Chung M.K. (1989) Lower back muscle forces in pushing and pulling. *Ergonomics* 32: 1552-1563.
24. Lee, P., Rogers, E., and Granata, K. P. Active Trunk Stiffness Increases with Co-Contraction. *J.Electromyo.Kinesiol.* 2004. Ref Type: In Press
25. Ljung,L. and Ljung,E.J. (1998) *System Identification: Theory for the User*, Prentice Hall, Upper Saddle River, NJ
26. Moorhouse, K. M. and Granata, K. P. Trunk stiffness and dynamics during active extension exertions. *J.Biomechanics* . 2004. Ref Type: In Press
27. Panjabi M.M. (1992) The stabilizing system of the spine. Part I Function, dysfunction, adaptation and enhancement. *J.Spinal Disorders* 5: 383-389.
28. Panjabi M.M. (1992) The stabilizing system of the spine. Part II Neutral zone and instability hypothesis. *J.Spinal Disorders* 5: 390-397.
29. Schibye B., Sogaard K., Martinsen D. and Klausen K. (2001) Mechanical load on the low back and shoulders during pushing and pulling of two-wheeled waste containers compared with lifting and carrying of bags and bins. *Clin.Biomech.* 16: 549-559.
30. Sinkjaer T., Toft E., Andreassen S. and Hornemann B.C. (1988) Muscle stiffness in human ankle dorsiflexors: Intrinsic and reflex components. *J.Neurophysiol.* 60: 1110-1121.

5.8 Figures

Figure 5.1. Experimental setup. Pseudo-random force perturbations were superimposed on isotonic loads applied to subjects to elicit small trunk movement. The external load acted anteriorly on the subject during an extension exertion trial in position shown. During a flexion exertion trial the subject faced away from the motor so that the external load acted posteriorly on the subject. Subjects were securely strapped into a rigid pelvic support structure to isolate movement of the trunk for all trials.

Figure 5.2. Typical IRF relating trunk displacement to the applied trunk force. Superimposed on the data is the least-mean-squares fits of the second-order parametric model. Parametric model coefficients represent effective trunk stiffness, damping and mass.

Figure 5.3. Normalized EMG activity was greater in three of the four bilateral muscle groups during flexion than during extension exertions. * indicates significance.

Figure 5.4. Trunk stiffness was significantly greater during flexion exertions than during extension exertions. This difference was attributed to co-contraction during flexion tasks. Stiffness increased significantly with exertion level.

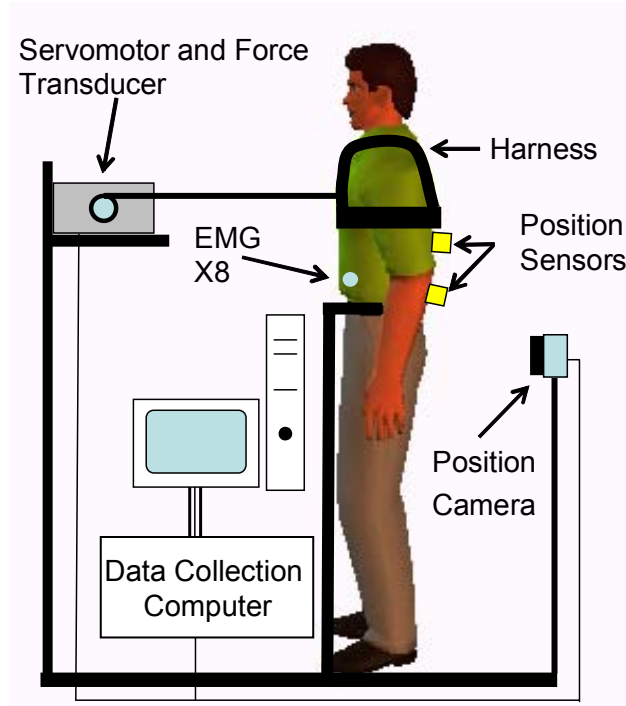


Figure 5.1. Experimental setup. Pseudo-random force perturbations were superimposed on isotonic loads applied to subjects to elicit small trunk movement. The external load acted anteriorly on the subject during an extension exertion trial in position shown. During a flexion exertion trial the subject faced away from the motor so that the external load acted posteriorly on the subject. Subjects were securely strapped into a rigid pelvic support structure to isolate movement of the trunk for all trials.

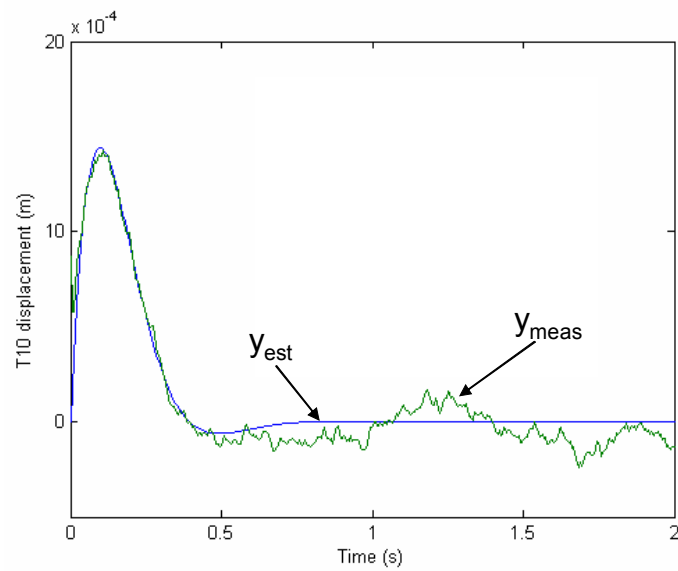


Figure 5.2. Typical IRF relating trunk displacement to the applied trunk force. Superimposed on the data is the least-mean-squares fits of the second-order parametric model. Parametric model coefficients represent effective trunk stiffness, damping and mass.

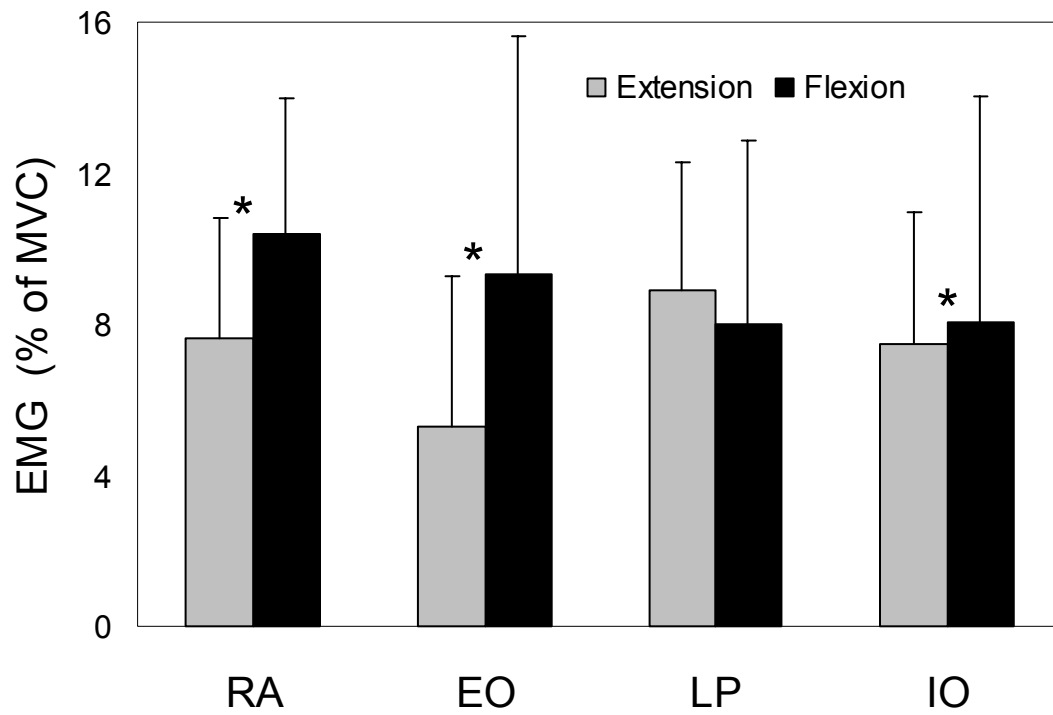


Figure 5.3. Normalized EMG activity was greater in three of the four bilateral muscle groups during flexion than during extension exertions. * indicates significance.

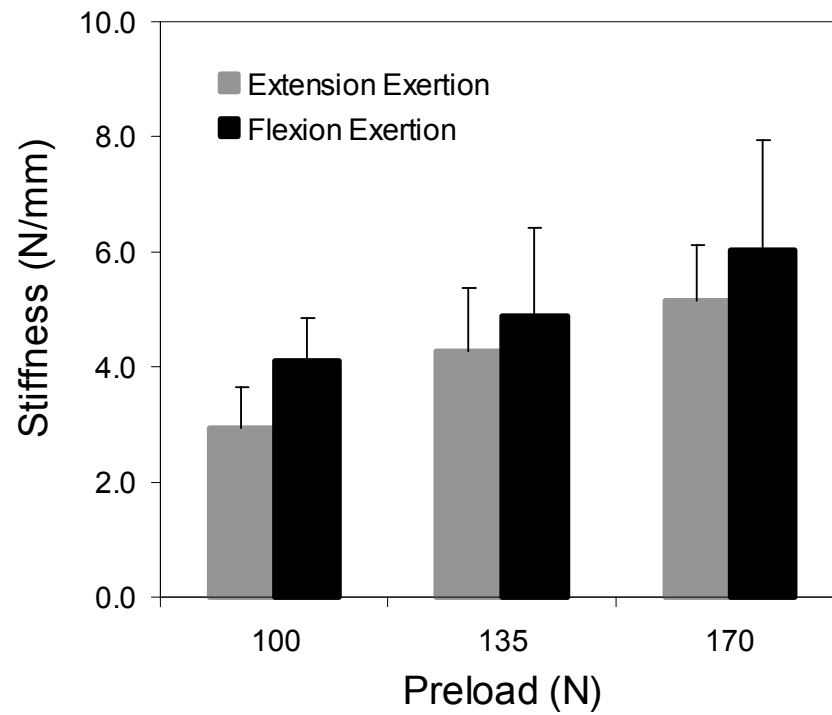


Figure 5.4. Trunk stiffness was significantly greater during flexion exertions than during extension exertions. This difference was attributed to co-contraction during flexion tasks. Stiffness increased significantly with exertion level.

CONCLUSIONS

Low back biomechanics during pushing and pulling tasks were investigated in this study. The results of this study have demonstrated that isometric pushing exertions are associated with significantly greater levels of co-contraction than isometric pulling exertions. Theoretical analysis in this study attributed co-contraction during pushing exertions as necessary to maintain stability of the spine. Empirical results indicated trunk co-contraction was shown to be associated with higher trunk stiffness. Trunk stiffness was shown to be higher during flexion exertions compared to extension exertions.

Results underscore the need to consider co-contraction and neuromuscular control of spinal stability when evaluating the biomechanical risks of pushing and pulling tasks. During extension tasks muscle recruitment directly contributes to spinal stability. During flexion tasks augmented recruitment patterns are necessary to maintain spinal stability. Results may indicate greater risk of spinal instability from motor control error during pushing tasks than pulling exertions.

Future studies need to consider the role of co-contraction contributions to spinal load during analyses of workplace pushing and pulling exertions. Past studies evaluating spinal compression during pushing exertions may have underestimated spinal compression because the significant effect of co-contraction was not accounted for. Although this study has provided insight into how the spine maintains stability spinal stability was not quantified. To the author's knowledge there are no existing quantitative measures of spinal stability. Further research is necessary to quantify the stability of the spine. The analyses in this study represent static exertions. Further research is necessary to quantify the role of dynamic flexion tasks on muscle recruitment, spinal load and

stability during pushing and pulling exertions.

Biomechanical understanding of the low back can be a useful tool for the prevention of LBDs. It is the hope of the author that the findings of this study contribute to the control of injuries in the future. Pushing exertions may be more of a biomechanical risk factor than pulling due to the elevated neuromuscular behavior needed during pushing to maintain spinal stability.

Appendix A – IRB Approval Form



Institutional Review Board

Dr. David M. Moore
IRB (Human Subjects) Chair
Assistant Vice President for Research Compliance
CVM Phase II- Duckpond Dr., Blacksburg, VA 24061-0442
Office: 540/231-4991; FAX: 540/231-6033
email: moored@vt.edu

DATE: December 22, 2004

MEMORANDUM

TO: Kevin P. Granata Engineering Science & Mechanics 0219

FROM: David Moore

SUBJECT: **IRB Expedited Continuation:** "Musculoskeletal Biomechanics of Movement and Control " IRB # 04-635 ref 03-632

This memo is regarding the above referenced protocol which was previously granted expedited approval by the IRB on January 21, 2004. The proposed research is eligible for expedited review according to the specifications authorized by 45 CFR 46.110 and 21 CFR 56.110. Pursuant to your request of last week, as Chair of the Virginia Tech Institutional Review Board, I have granted approval for extension of the study for a period of 12 months, effective as of January 21, 2005.

Approval of your research by the IRB provides the appropriate review as required by federal and state laws regarding human subject research. It is your responsibility to report to the IRB any adverse reactions that can be attributed to this study.

To continue the project past the 12-month approval period, a continuing review application must be submitted (30) days prior to the anniversary of the original approval date and a summary of the project to date must be provided. Our office will send you a reminder of this (60) days prior to the anniversary date.

Virginia Tech has an approved Federal Wide Assurance (FWA00000572, exp. 7/20/07) on file with OHRP, and its IRB Registration Number is IRB00000667.

cc: File

Appendix B – Consent Forms

Title of Project: Musculoskeletal Biomechanics of Movement and Control

Investigators: **K.P. Granata**

Purpose of this Research

To understand musculoskeletal injury and improve clinical diagnoses of injury it is necessary to understand how muscles control force and movement. The purpose of this study is to measure the relation between human movement, force generation and muscle activity. We are also interested in observing how gender, fatigue and physical conditioning influence these parameters. Throughout the course of this project more than 200 subject volunteers will participate including healthy individuals from the age of 18 to 55.

Procedures

We will tape adhesive markers and sensors on your skin around your trunk, legs and arms. These sensors are EMG electrodes that measure the activity of your muscles and position sensors to measure how you move. After some preliminary warm up stretches, we may ask you to push and/or pull as hard as you can against a resistance. We may then ask you to hold or lift a weight or weighted-box and to bend forward and back. We may also ask you to do some fatiguing exertions such as holding or lifting a heavy weight or pushing/pulling against a bar or cable for several minutes. We may also apply a quick but small force to record reflexes. You may be requested to return for repeated testing. Between test sessions you may be asked to participate in specified physical conditioning as per the American College of Sports Medicine recommended guidelines

Risks

The risks of this study are minor. They include a potential skin irritation to the adhesives used in the tape and electrode markers. You may also feel some temporary muscle soreness such as might occur after exercising. Subjects participating in physical conditioning may experience muscle soreness and/or musculoskeletal injury associated with inherent risks of cardiovascular, strength training and therapeutic exercise. To minimize these risks you will be asked to warm-up before the tasks and tell us if you are aware of any history of skin-reaction to tape, history of musculoskeletal injury, cardiovascular limitations.

Benefits

By participating in this study, you will help to increase our understanding musculoskeletal control of movement and musculoskeletal injury mechanisms. We hope to make this research experience interesting and enjoyable for you where you may learn experimental procedures in biomechanical sciences. We do not guarantee or promise that you will receive any of these benefits and no promise of benefits has been made to encourage your participation.

Anonymity and Confidentiality

Experimental data collected from your participation will be coded and matched to this consent form so only members of the research team can determine your identity. Your identity will not be divulged to unauthorized people or agencies. Digital video recorded during the experimental trials will be used to track the movement of the sensors by means of computer analyses and is insufficient video quality to observe individual participant identifying characteristics. Secondary VHS-style video may be recorded to validate the digital motion data. This camera angle is placed to avoid facial or other identifying characteristics. Sometimes it is necessary for an investigator to break confidentiality if a significant health or safety concern is perceived or the participant is believed to be a threat to himself/herself or others.

Compensation

Participants required to return for multiple test sessions or participate in physical conditioning for this protocol will receive payment per the number of test sessions as well as a bonus for full completion of the multi-session research protocol. Subjects participating in experiments as part of course or laboratory procedures will receive appropriate credit for analysis of specified data as described in the course syllabus but not for personal performance during the experimental session. If course credit is involved and the subject chooses not to

participate alternative means for earning equivalent credit will be established with the course instructor.

Freedom to Withdraw

You are free to withdraw from a study at any time without penalty. If you choose to withdraw, you will be compensated for the portion of the time of the study (if financial compensation is involved). If you choose to withdraw, you will not be penalized by reduction in points or grade in a course (if course credit is involved). You are free not to answer any questions or respond to experimental situations that they choose without penalty.

There may be circumstances under which the investigator may determine that you should not continue as a subject. You will be compensated for the portion of the project completed

Approval of Research

This research project has been approved, as required, by the Institutional Review Board for Research Involving Human Subjects at Virginia Polytechnic Institute and State University, by the Department of Engineering science and Mechanics.

21 January 2003
IRB Approval Date

20 January 2004
Approval Expiration Date

Subject's Responsibilities

I voluntarily agree to participate in this study. I have the following responsibilities:

- Inform the investigators of all medical conditions that may influence performance or risk
- Comply to the best of my ability with the experimental and safety instructions
- Inform the investigator of any physical and mental discomfort resulting from the experimental protocol

Subject's Permission

I have read and understand the Informed Consent and conditions of this project. I have had all my questions answered. I hereby acknowledge the above and give my voluntary consent:

Subject Name (Print): _____

Subject signature: _____

Date _____

_____ Date _____
Witness (Optional except for certain classes of subjects)

Should I have any pertinent questions about this research or its conduct, and research subjects' rights, and whom to contact in the event of a research-related injury to the subject, I may contact:

Investigator(s): Patrick Lee E-mail: palee2@vt.edu Phone 231-2022
Faculty Advisor: K.P. Granata E-mail: Granata@vt.edu Phone 231-7039

Departmental Reviewer/Department Head

Telephone/e-mail

David M. Moore
Chair, IRB
Office of Research Compliance
Research & Graduate Studies

Subjects must be given a complete copy (or duplicate original) of the signed Informed Consent

Appendix C – Data Collection Forms

Data Collection Form for Study 1&3

CO-CONTRACTION AS A FUNCTION OF LOAD DIRECTION
TRUNK STIFFNESS AS A FUNCTION OF LOAD DIRECTION

Subject # _____
Name: _____

Max files EMG files: 1,2,3,4,5,6
Perturbation of 35 N on each trial

Flexion

Trial	Actual	Bias	Comments	File #
7		100		1
8		135		2
9		135		3
10		100		4
11		170		5
12		135		6
13		170		7
14		170		8
15		100		9

Extension

Trial		Bias	Comments	File #
16		170		1
17		135		2
18		135		3
19		100		4
20		170		5
21		100		6
22		100		7
23		135		8
24		170		9

Data Collection Form for Study 2

TRUNK STIFFNESS AS A FUNCTION OF CO-ACTIVATION

Subject #		
EMG Max trials	s###max1...6	
Max Exertion (N)		
		Preload 1: 15% MAX (N)
		Preload 2: 30% MAX (N)

Co-Contraction	Preload	Filename
OFF	2	
	1	s###OFFbias#tr#
	1	
	2	
ON	1	
	2	s###ONbias#tr#
	1	
	2	

Vita

Patrick James Lee

Patrick Lee was born in Baltimore, Maryland on October 12, 1980. He attended Centennial High School in Ellicott City, MD. He graduated from Virginia Polytechnic and State University. Tech with a Bachelor's in Mechanical Engineering in 2002. He continued his studies at Virginia Polytechnic and State University and obtained a Master's in Mechanical Engineering in 2004. His research work conducted at the Musculoskeletal Biomechanics Lab was published in national and international journal publications. The focus of his research was low back biomechanical analysis of occupational tasks associated with a risk of injury; pushing, pulling, and twisting exertions. During his free time, Patrick enjoys reading and outdoor activities such as bicycling, hiking, and snowboarding.